Micro-trench measurements at DIII-D DiMES divertor surface to investigate ion incident angles, sheath length, and erosion

S. Abe*[a], C.H. Skinner[b], B.E. Koel[a],
I. Bykov[c], D. Rudakov[d], A. Lasa[e] J. Guterl[c],
J. Coburn[f], Y.W. Yeh[g], C.J. Lasnier[h],
A.G. McLean[h], H.Q. Wang[c], T. Abrams[c]

[a]PU, [b]PPPL, [c]GA, [d]UCSD, [e]UTK, [f]Sandia, [g]Rutgers, [h]LLNL

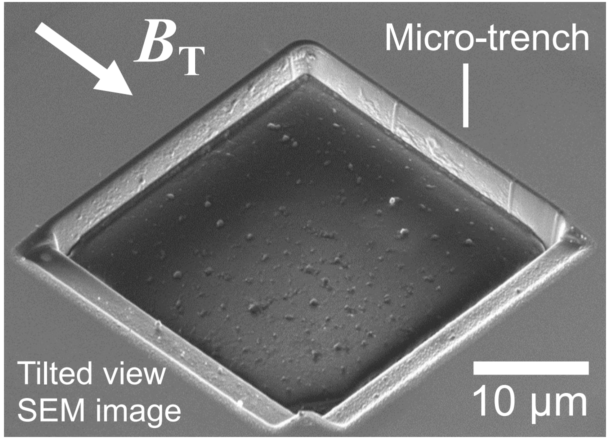

NSTX-U / Magnetic Fusion Science meeting

11/29/2021

Ion incident direction is critical parameter for PFC lifetime

Both **polar** and **azimuthal** Ion incident angles affect erosion and migration

Strong dependency on incident angle

Fusion reactor B field

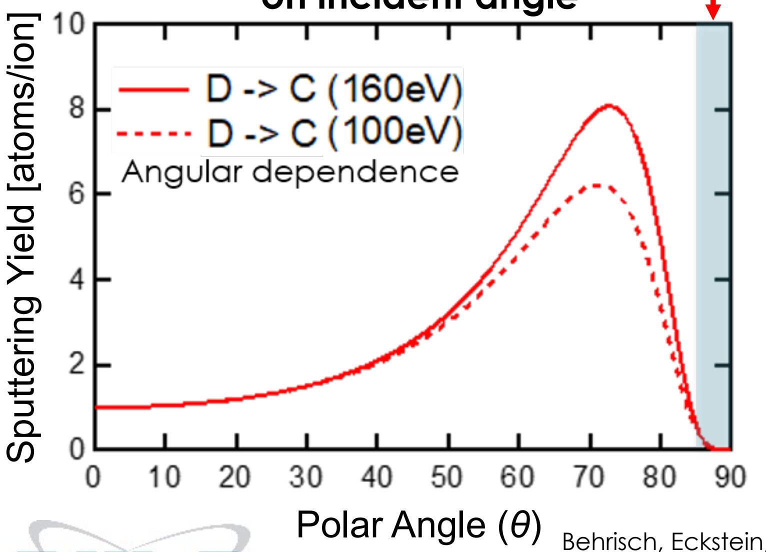

Behrisch, Eckstein, "Sputtering by Particle Bombardment" (2007)

Rough & Anisotropic surface of SiC DIII-D DiMES sample

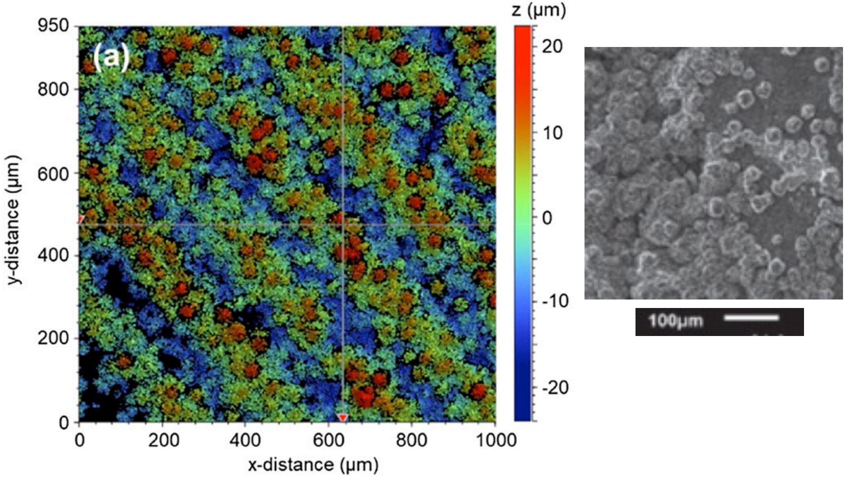

Abrams et al., NF 2021

Sheath width is a critical parameter of the sheath structure

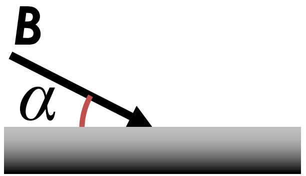

- Classical Debye sheath (DS) vanishes when $\alpha < 5°$
- **Wide electric sheath**, magnetic pre-sheath (**MPS**) or Chodura sheath : $L_{MPS} \sim \rho_i$

Sheath structure affects:

- Ion trajectories, i.e. **impact angle**
  Chrobak NF 2018
- Prompt redeposition
  Guterl NME 2021, Stangeby NF 2021
  Tskhakaya JNM 2015

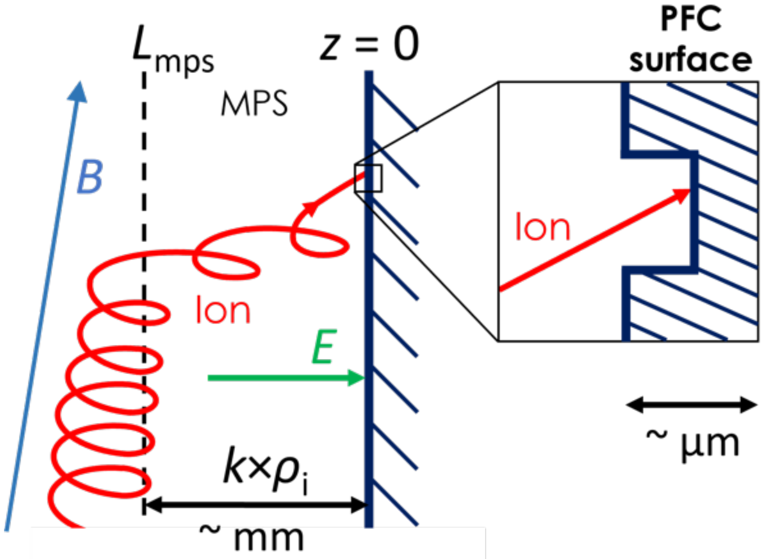

Sheath width is a critical parameter of the sheath structure

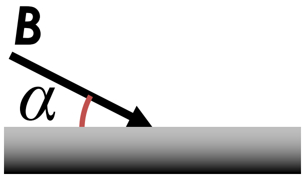

- Classical Debye sheath (DS) vanishes when $\alpha < 5°$
- **Wide electric sheath**, magnetic pre-sheath (**MPS**) or Chodura sheath : $L_{MPS} \sim \rho_i$

Sheath structure affects:

- Ion trajectories, i.e. impact angle
  Chrobak NF 2018
- **Prompt redeposition**
  Guterl NME 2021, Stangeby NF 2021
  Tskhakaya JNM 2015

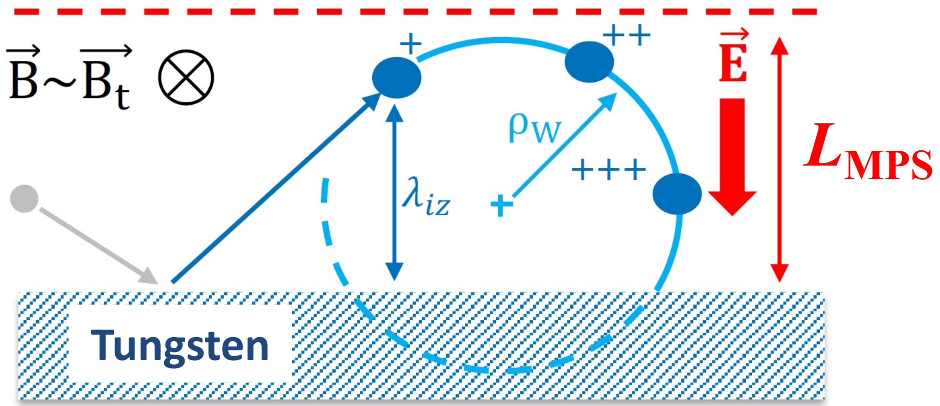

Multiple ionizations of W impurities *in the sheath* Guterl NME 2021

Sheath width is a critical parameter of the sheath structure

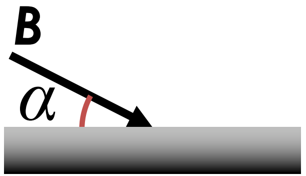

- Classical Debye sheath (DS) vanishes when **α < 5º**
- **Wide electric sheath**, magnetic pre-sheath (**MPS**) or Chodura sheath : $L_{MPS} \sim \rho_i$

Coulette PPCF 2016

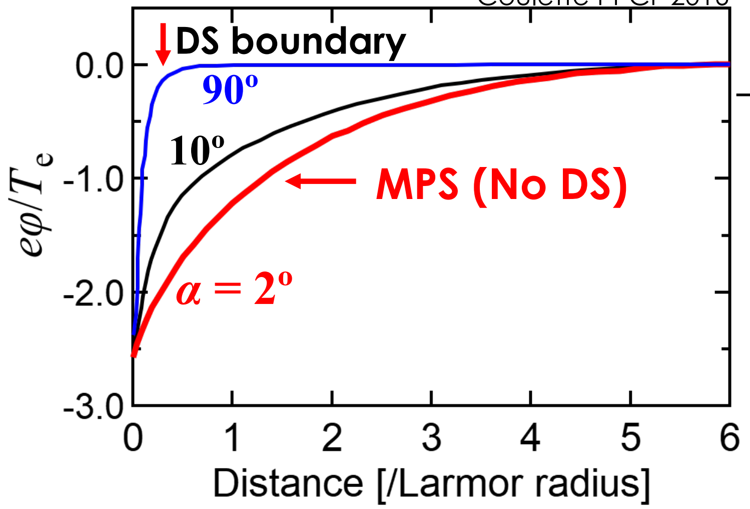

Sheath potential profile calculated by **kinetic simulation**

Sheath width is a critical parameter of the sheath structure

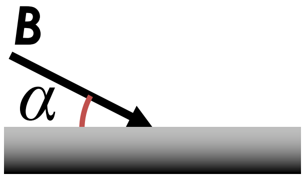

- Classical Debye sheath (DS) vanishes when $\alpha < 5^{\circ}$
- **Wide electric sheath**, magnetic pre-sheath (**MPS**) or Chodura sheath : $L_{MPS} \sim \rho_i$

Coulette PPCF 2016

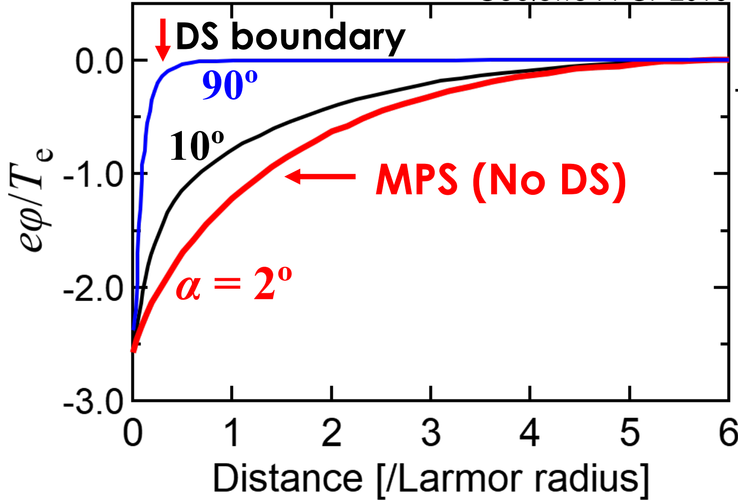

Sheath potential profile calculated by **kinetic simulation**

Potential profile is well approximated by **exponential function**

$$\phi(z) = \Lambda T_e e^{-\frac{2z}{L_{MPS}}}$$

$(-3 < \Lambda < -2.4)$

Borodkina CPP 2016
Stangeby 2000 IOP Publishing

$L_{MPS} = k \times \rho_i$ (ρ_i: Ion gyro radius)

$k \sim$ **2-3** by theoretical studies for conventional Tokamak and ITER-like parameters

Stangeby NF 2012,
Coulette PPCF 2016,
Chodura PF 1982

Sheath width is a critical parameter of the sheath structure

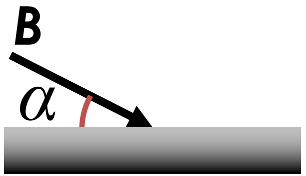

- Classical Debye sheath (DS) vanishes when $\alpha < 5^o$
- **Wide electric sheath**, magnetic pre-sheath (**MPS**) or Chodura sheath : $L_{MPS} \sim \rho_i$

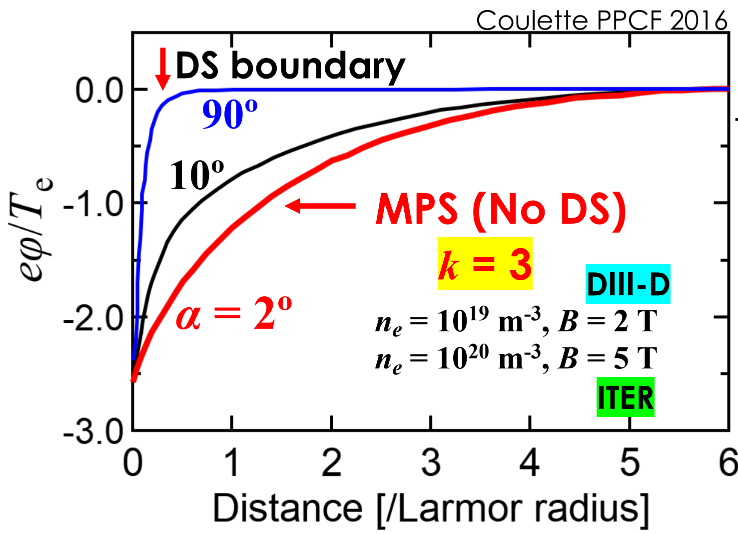

Sheath potential profile calculated by **kinetic simulation**

Potential profile is well approximated by **exponential function**

$$\phi(z) = \Lambda T_e e^{-\frac{2z}{L_{MPS}}}$$

$(-3 < \Lambda < -2.4)$

Borodkina CPP 2016
Stangeby 2000 IOP Publishing

$L_{MPS} = k \times \rho_i$ (ρ_i: Ion gyro radius)

$k \sim 2\text{-}3$ by theoretical studies for conventional Tokamak and ITER-like parameters

Stangeby NF 2012, Coulette PPCF 2016, Chodura PF 1982

DIII-D NATIONAL FUSION FACILITY SAN DIEGO

Ion trajectory tracing for Ion Angle Distributions (IADs)

Ion trajectory in sheath calculated by

Equation-of-motion (EOM) Chrobak NF 2018 Schmid NF 2010

$$\boldsymbol{F} = e(\boldsymbol{E} + \boldsymbol{v} \times \boldsymbol{B})$$

using

$$\phi(z) = \Lambda T_e \mathrm{e}^{-\frac{2z}{k \times \rho_i}}$$

and **initial velocity distribution**

$v_{0,\perp}$: Maxwell-Boltzmann ($T_e = T_i$)

$v_{0,\parallel}$: Top-hat up to $\sqrt{2kT_e/m_i}$ (width $\sqrt{kT_i/m_i}$)

Collisionless assumption: L_{MPS} (~ mm) << λ_{MFP} (~cm)

DIII-D divertor plasmas, $n_e = 10^{19}$ m^{-3}

*However, $\lambda_{ChargeExchange}$ ~ 0.1 mm when $n_e = n_n = 10^{21}$ m^{-3}

ITER

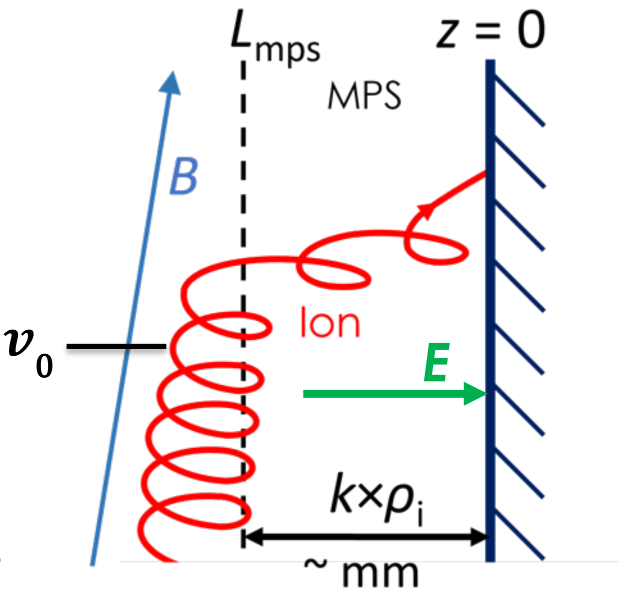

Equation-of-motion model

Ion trajectory in sheath

DIII-D NATIONAL FUSION FACILITY SAN DIEGO

Ion angle distributions (IADs) can reveal sheath structure

DIII-D attached deuterium L-mode plasma
$T_e \sim 30$ eV, $n_e \sim 10^{19}$ m^{-3}, $\alpha = 1.5°$

IADs by Equation-of-Motion

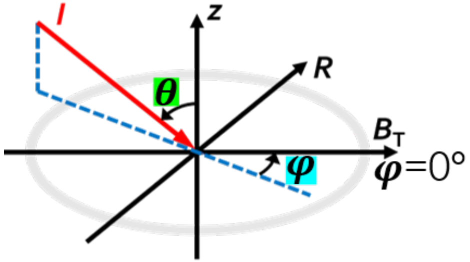

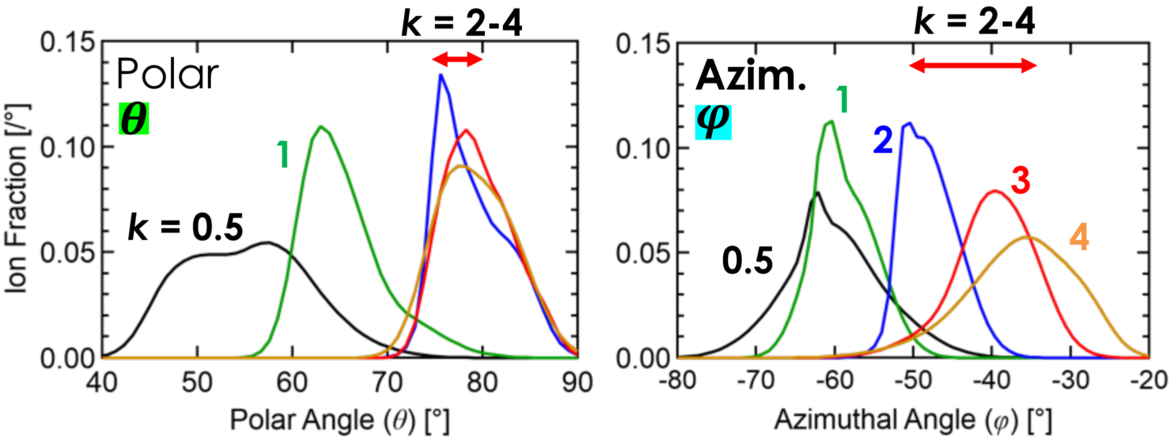

***k* ~ 3** by kinetic model
Coulette PPCF 2016

GOAL:

Measuring **azimuthal IAD** & Determining L_{MPS} $(= k \times \rho_i)$

Engineered samples exposed on DiMES

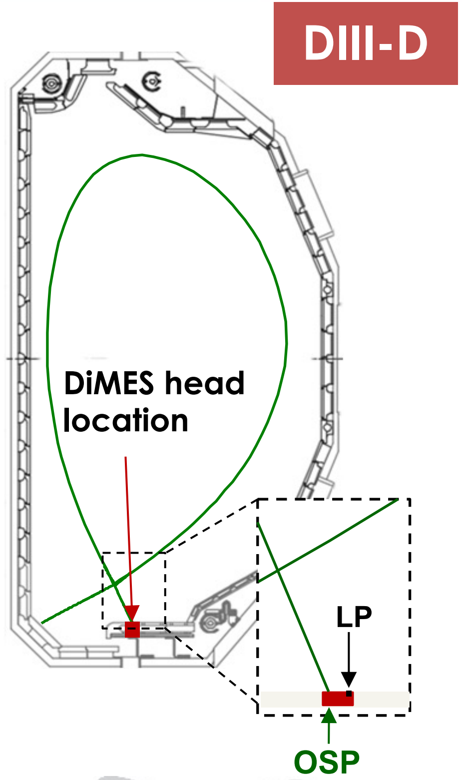

Plasma parameters

DIII-D attached deuterium L-mode plasma
$T_e \sim 30$ eV, $n_e \sim 10^{19}$ m^{-3}, $I_{\perp} \sim 10^{22}$ m^{-2}s^{-1},
$t_{exp} = 10$ s , $T_{surf} < 250$ °C

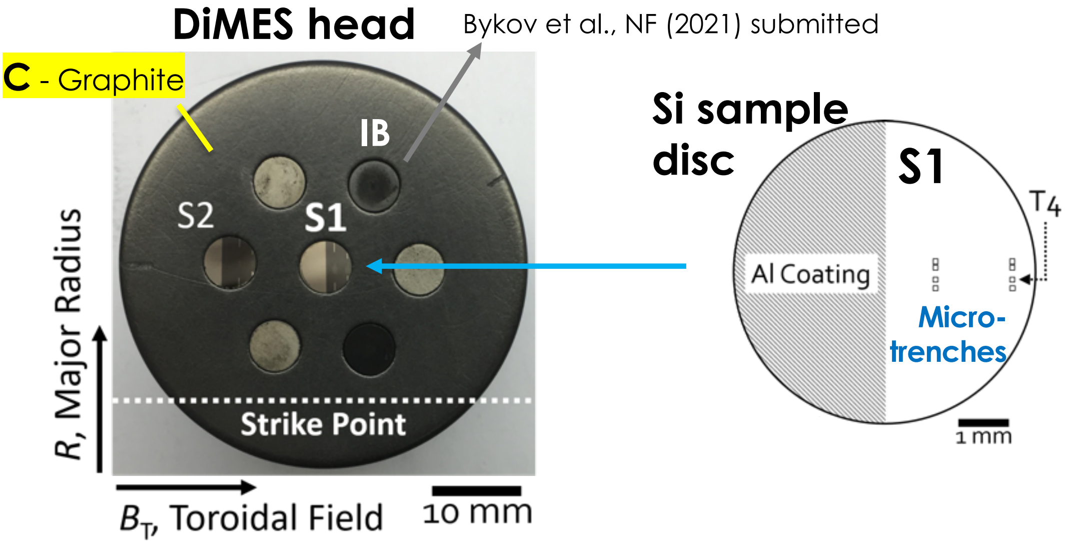

Micro-trench technique uses ion shadowing effect to reveal D ion incident direction

Micro trenches fabricated by focused ion (Ga) beam (FIB)

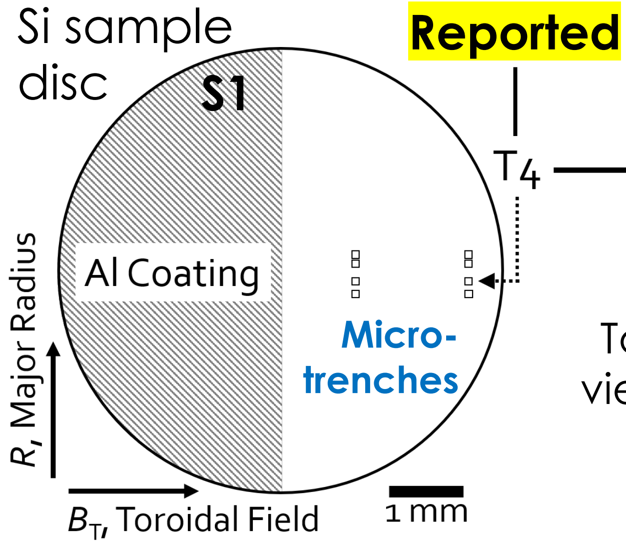

SEM before exposure

30x30x4 μm deep

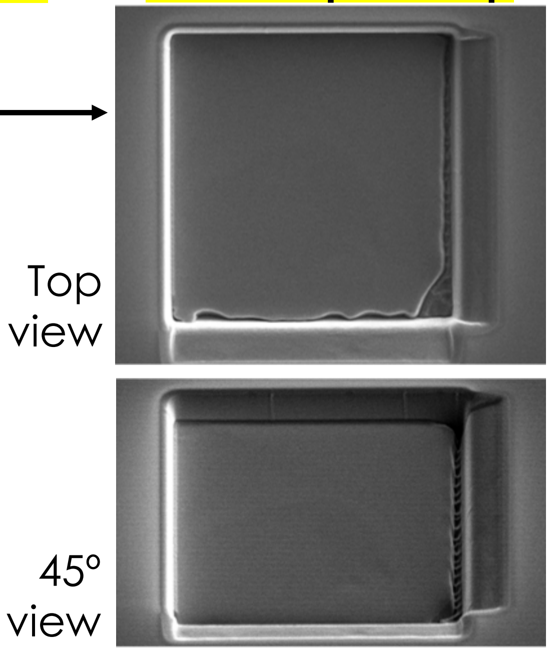

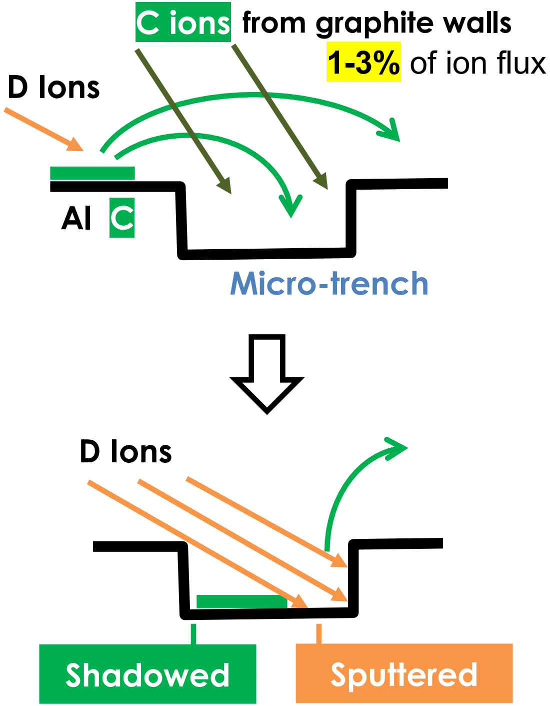

S. Abe 2021 NME **27** 100965

Uniform C gross deposition expected for D ion irradiated area

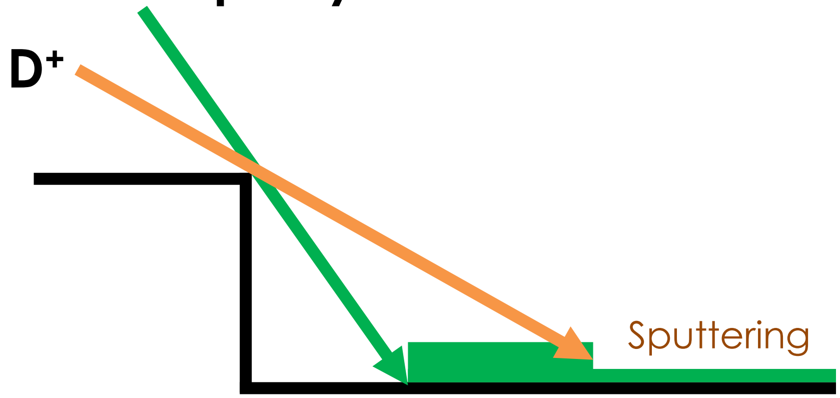

Determining D ion directions by impurity net deposition pattern

Requirements:

- D ion irradiated area is included in impurity re-deposited area
- C gross deposition is uniform

Polar angle θ prediction:

	Prompt redeposition C^+, Al^+		C^+		D^+	
Steep	20-45°	<	60°	<	80°	Shallow
	Brooks, FED 2002		Measured &Predicted		Bykov, 2021 unpublished Abe, Phys. Scripta 2021	

D ion physical sputtering dominates C erosion

$T_e = T_i =$ **30 eV**

$\boldsymbol{E}_{\mathbf{ion}} = 3Z_iT_e + 2T_i$

=**150 eV** (Z_i = **1**)

~**300 eV** (Z_i = **3**)

Stangeby, IOP Publishing (2000)

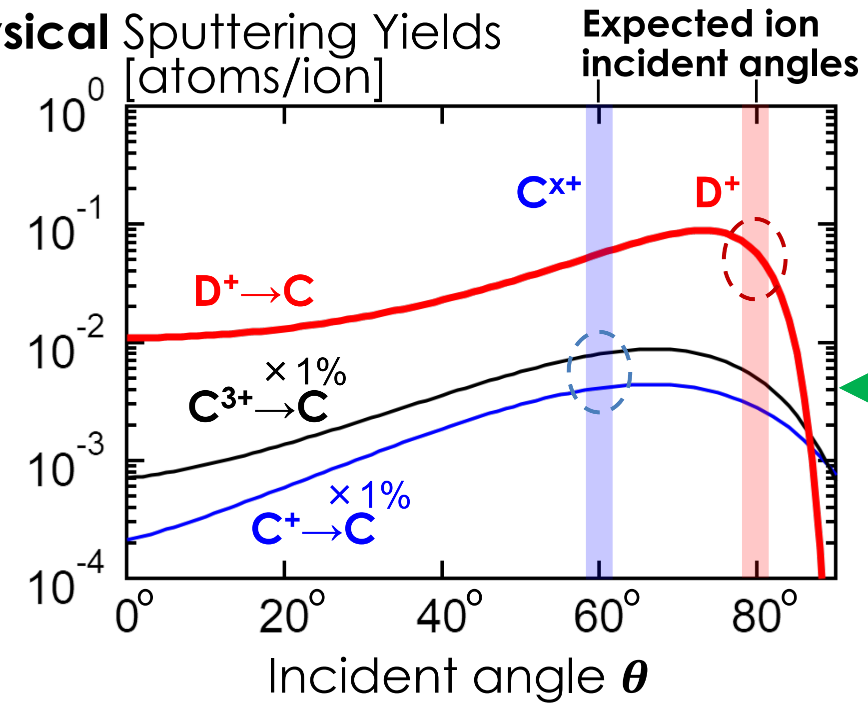

Chemical Erosion Yields

D^+

Y_{Chem}=**0.004**

(400-500 K)

Roth, JNM (1999)

Behrisch, Eckstein, "Sputtering by Particle Bombardment" 2007

$Y_{Phys}(D^+) \gg Y_{Phys}(C^{x+}) \times 1\% \sim Y_{Chem}(D^+)$

C concentration in ion flux

C erosion calculated by MPR (Micro-patterning and Roughness)

Lasa, Coburn, github.com/ORNL-Fusion/

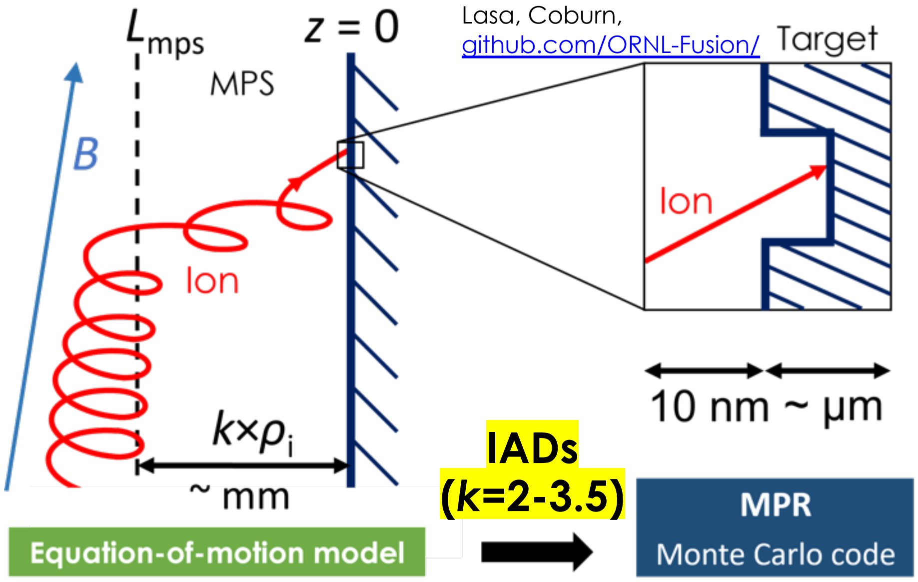

Calculated gross erosion [# particles/cell]

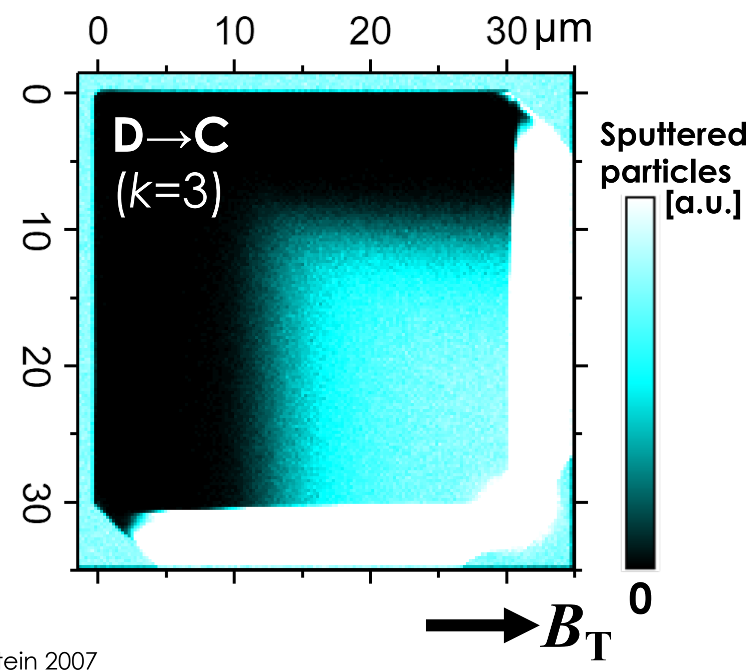

Other MPR inputs

- Trench geometry — Atomic force microscopy (AFM)
- Ion energy: 5 T_e = 150 eV
- Sputtering yields D→C — Behrisch, Eckstein 2007

DIII-D NATIONAL FUSION FACILITY SAN DIEGO

Impurities are redeposited and trapped in the D ion shadowed area

Before exposure

After exposure

SEM images

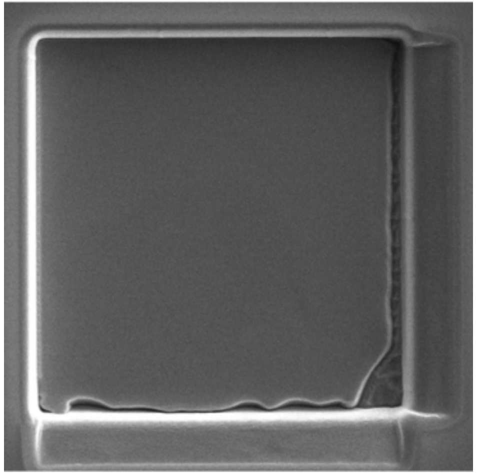

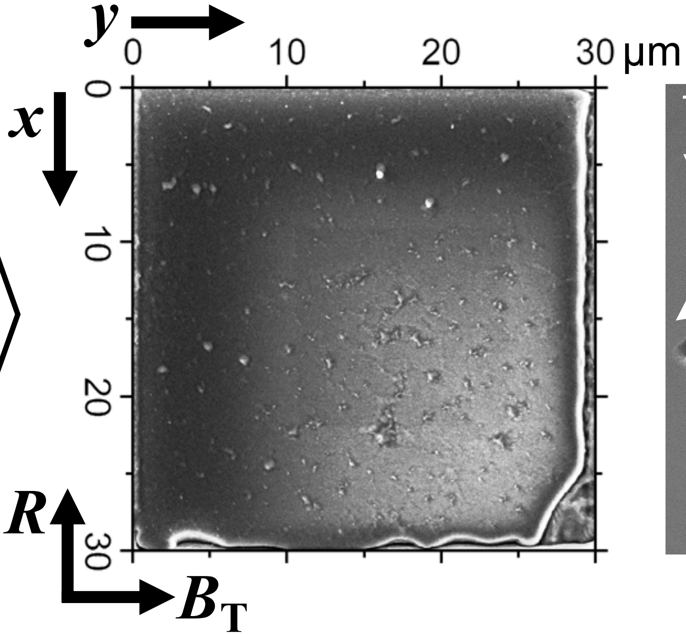

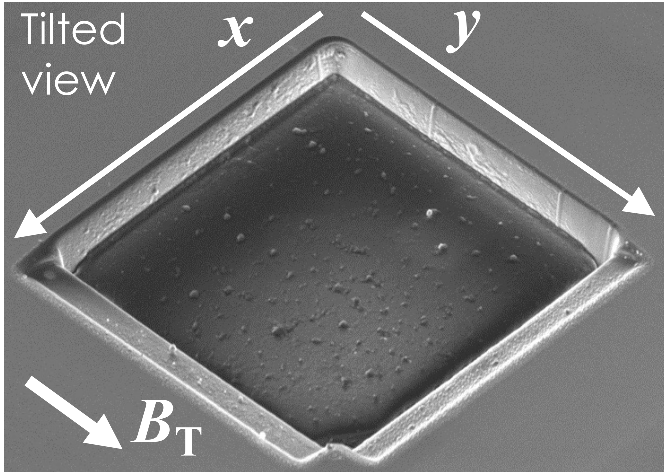

Dark area = impurity deposition

Energy dispersive X-ray spectroscopy (EDS) analysis revealed elemental maps of redeposited impurities

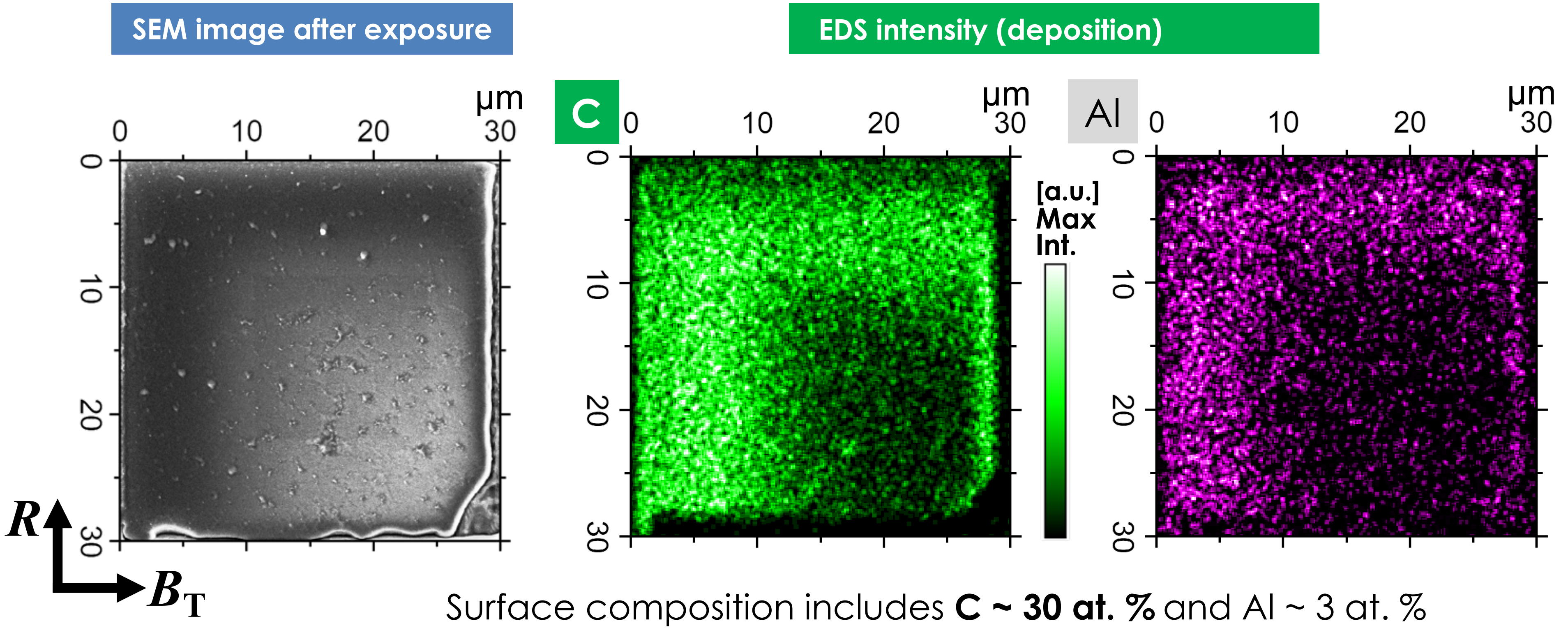

Surface composition includes **C ~ 30 at. %** and Al ~ 3 at. %

C intensity will be used for erosion simulation comparison

Energy dispersive X-ray spectroscopy (EDS) analysis revealed elemental maps of redeposited impurities

SEM image after exposure

EDS intensity (deposition) contours

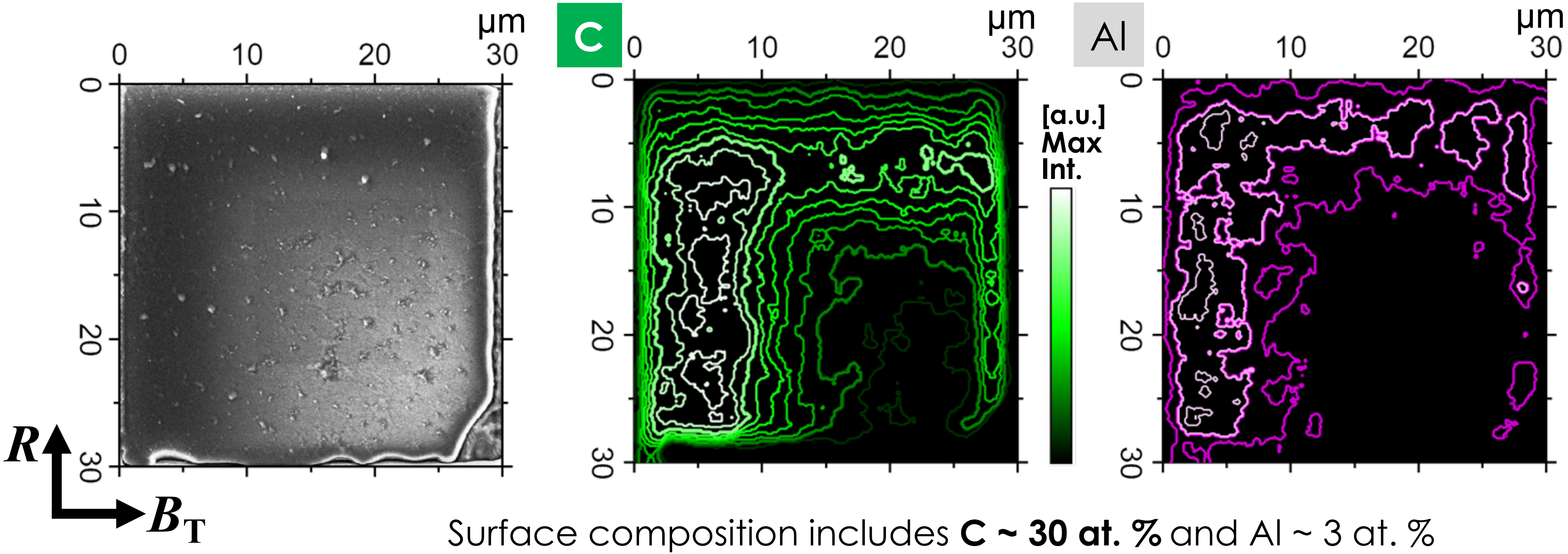

Surface composition includes **C ~ 30 at. %** and Al ~ 3 at. %

C intensity will be used for erosion simulation comparison

DIII-D NATIONAL FUSION FACILITY SAN DIEGO

Comparison of calculated and measured D→C sputtering patterns

Calculated gross erosion | **Sputtered particles** | **C deposition (exp.)**

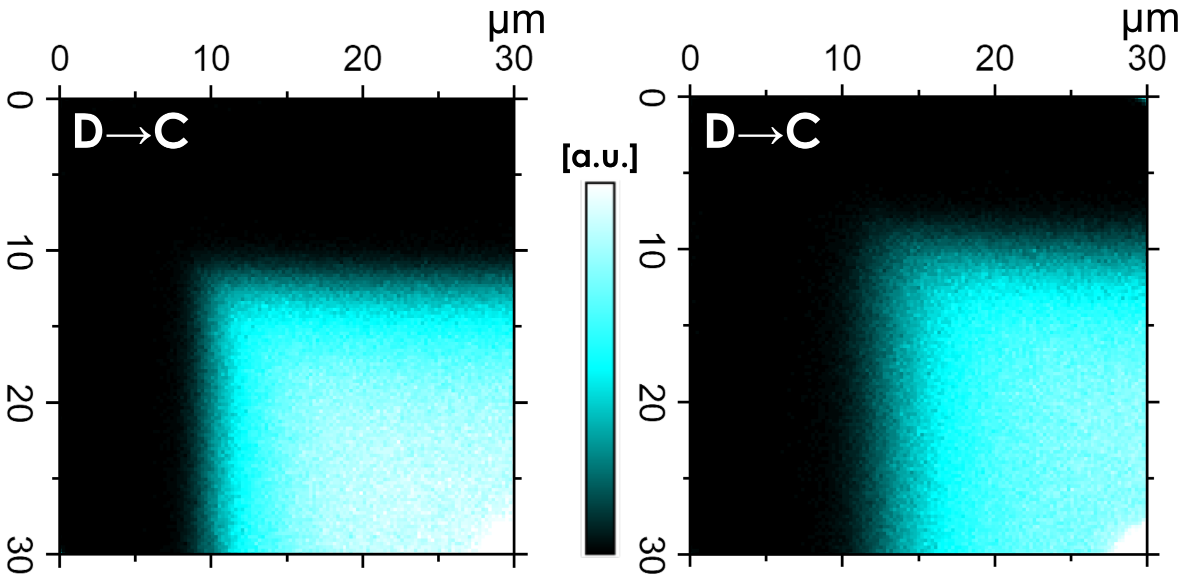

k = 2 $L_{MPS} = k \times \rho_i$ (ρ_i: Ion gyro radius) **k = 3**

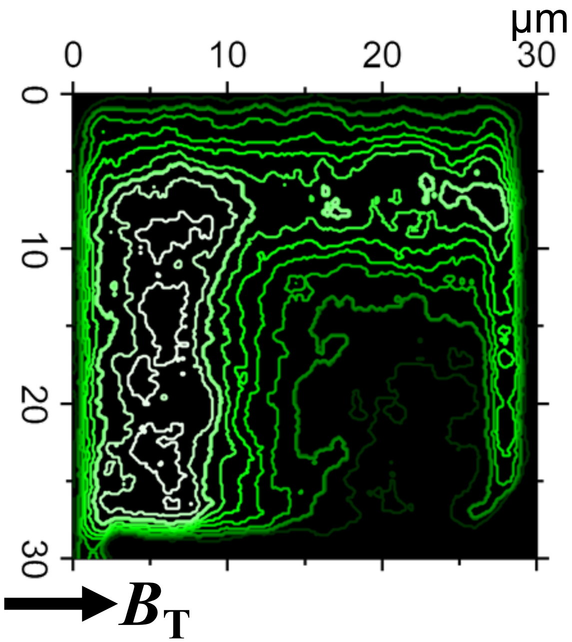

Calculated shadowed area for ***k* = 3** consistent with measured C

Comparison of calculated and measured D→C sputtering patterns

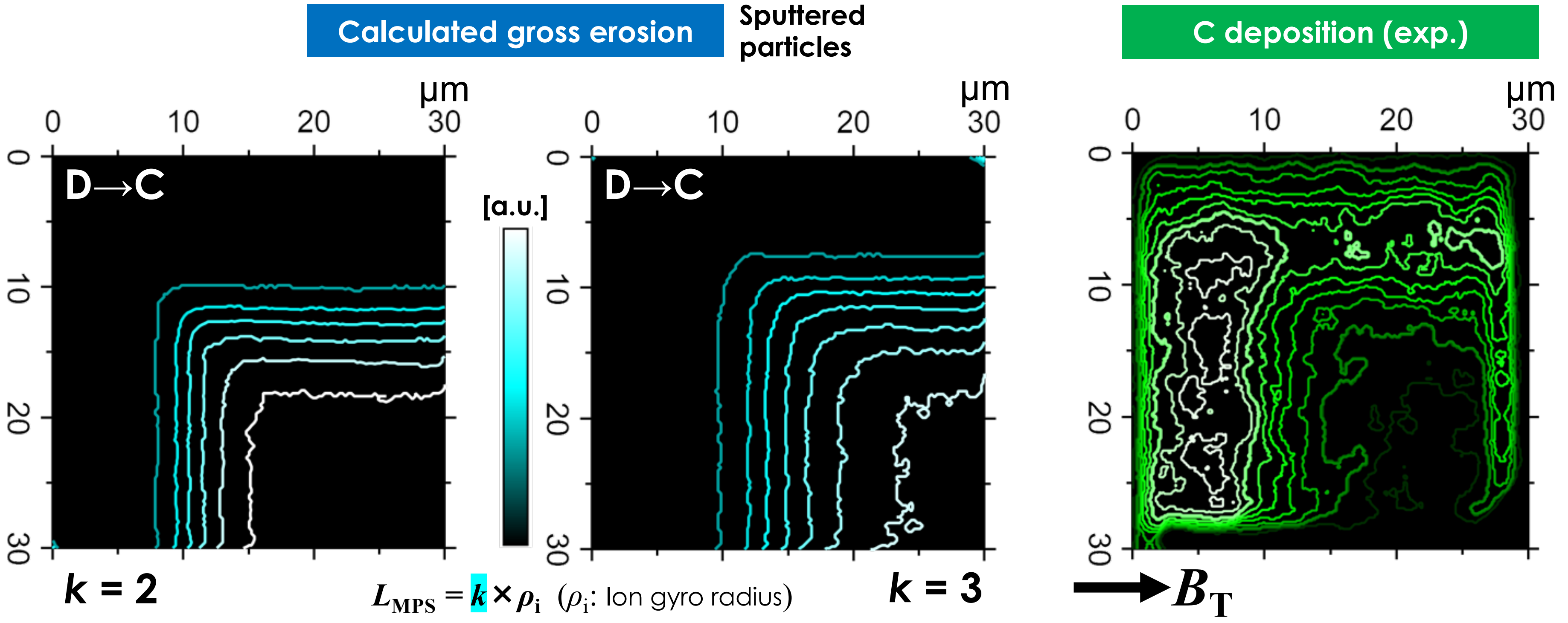

$L_{\mathrm{MPS}} = k \times \rho_{\mathrm{i}}$ (ρ_{i}: Ion gyro radius)

Calculated shadowed area for ***k* = 3** consistent with measured C

Comparison of calculated and measured D→C sputtering patterns

Calculated gross erosion

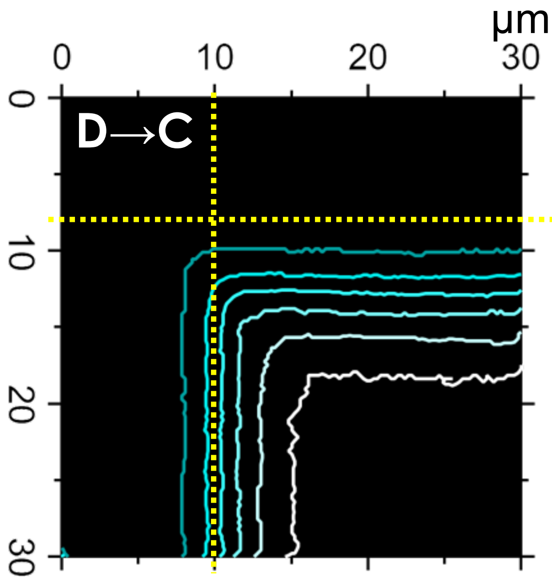

k = 2

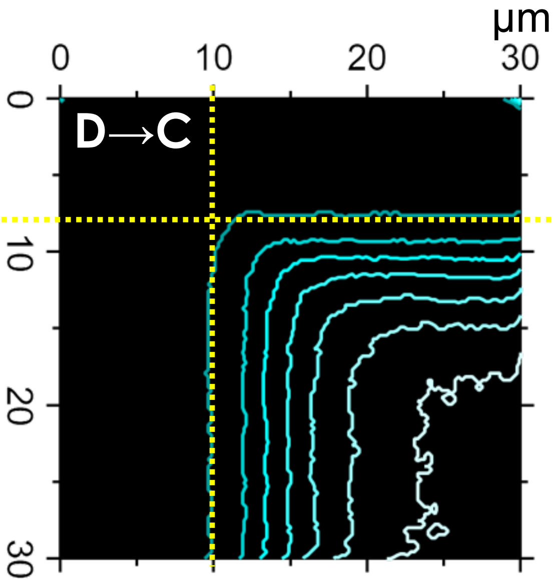

$L_{\mathrm{MPS}} = k \times \rho_i$ (ρ_i: Ion gyro radius)

k = 3

C deposition (exp.)

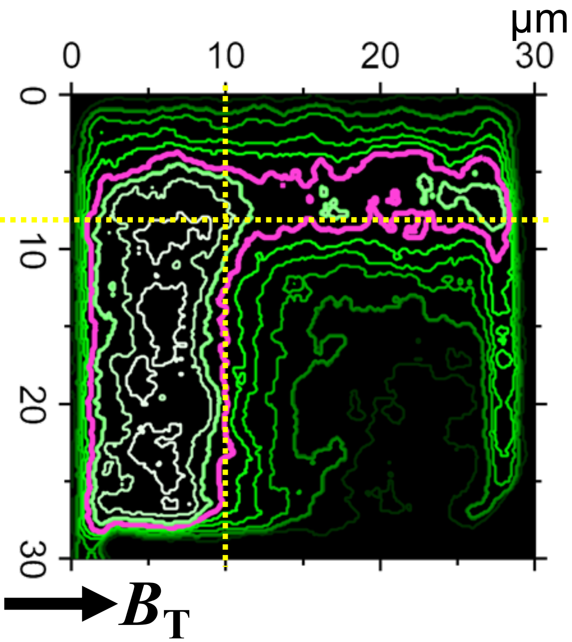

Calculated shadowed area for ***k* = 3** consistent with measured C

Comparison of calculated and measured D→C sputtering patterns

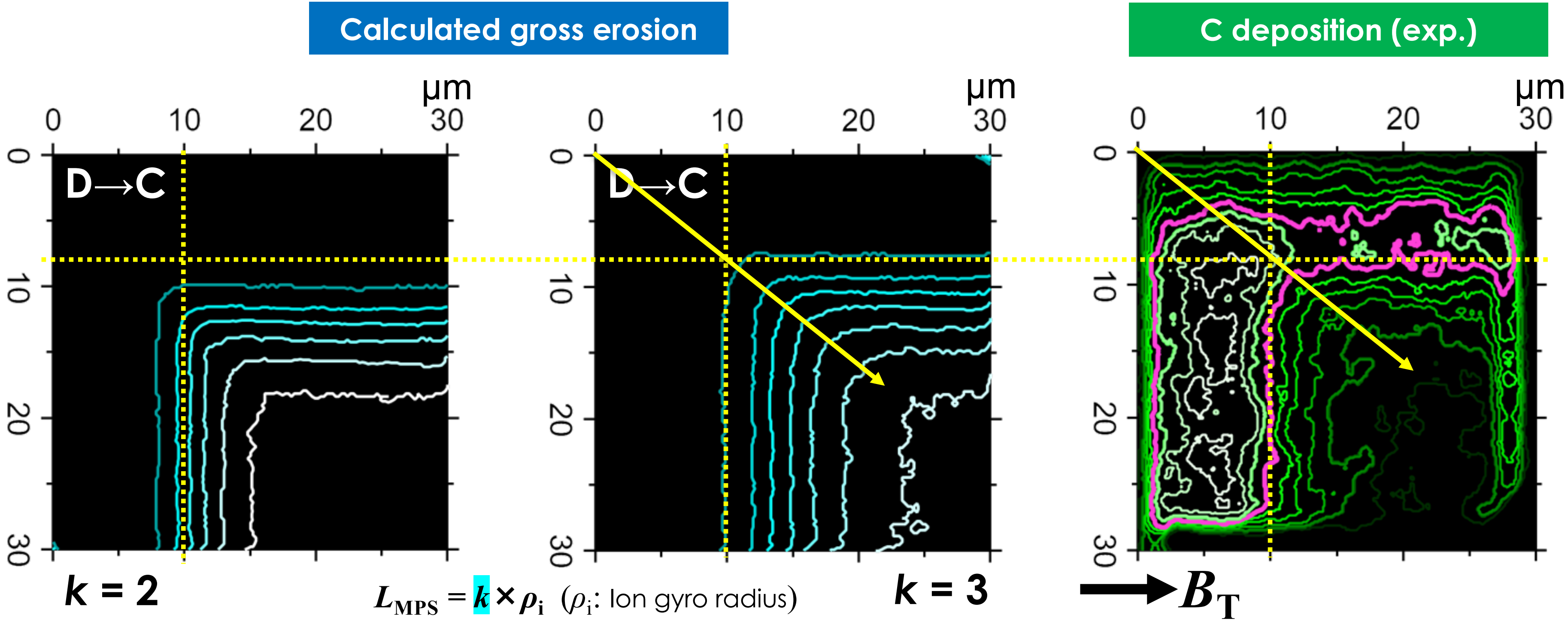

$L_{MPS} = k \times \rho_i$ (ρ_i: Ion gyro radius)

Calculated shadowed area for **k = 3** consistent with measured C

Erosion peak direction was clearly observed

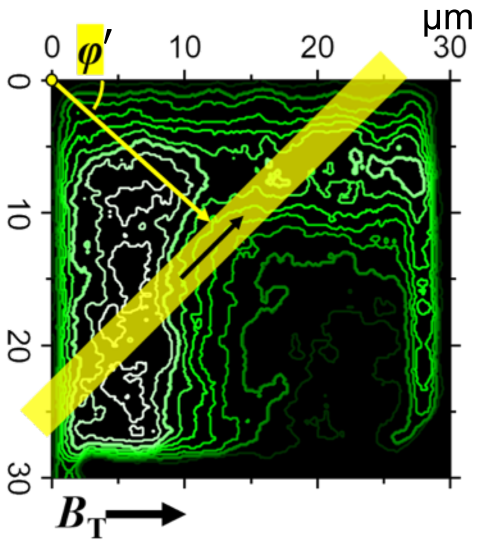

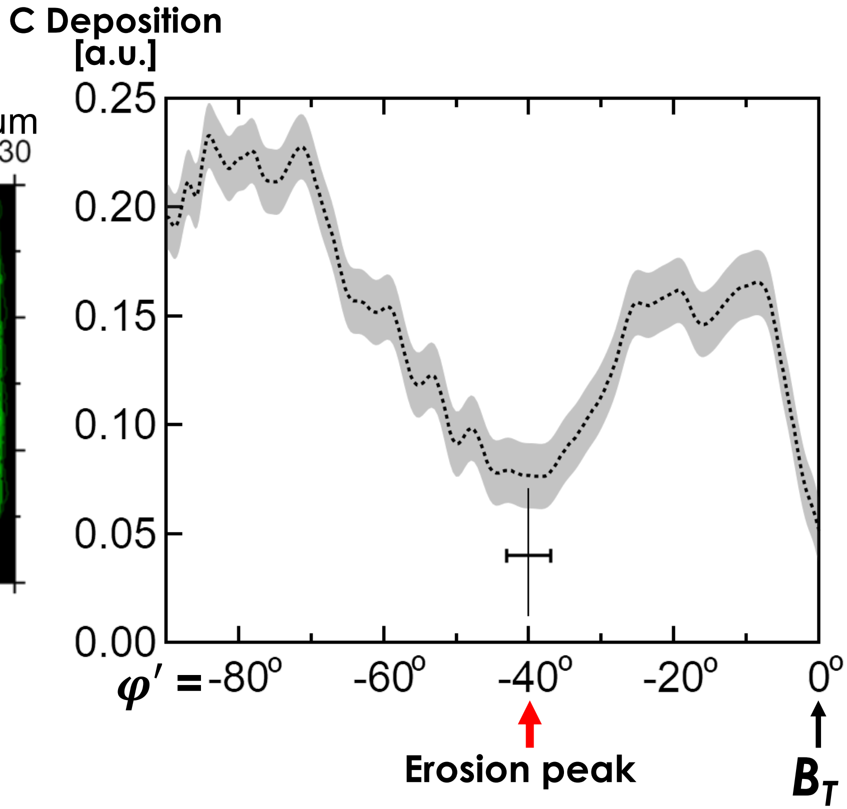

L_{MPS} (k) was determined by comparing with calculated erosion

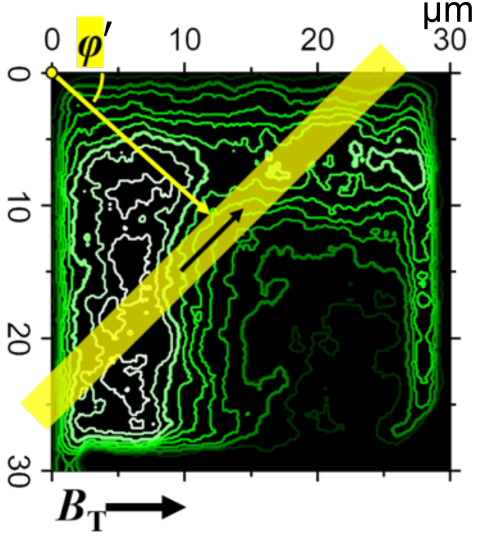

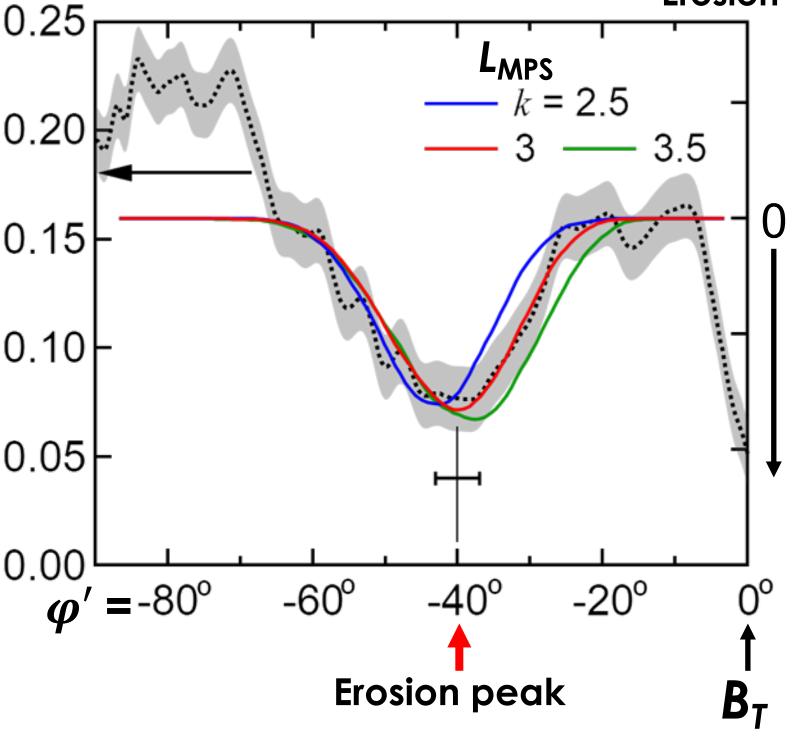

Good agreement is obtained for **k = 2.5-3.5**

$L_{MPS} = k \times \rho_i$ (ρ_i: Ion gyro radius)

giving azimuthal D ion direction

φ = -40°

Abe, NF 2021 accepted

L_{MPS} (k) was determined by comparing with calculated erosion

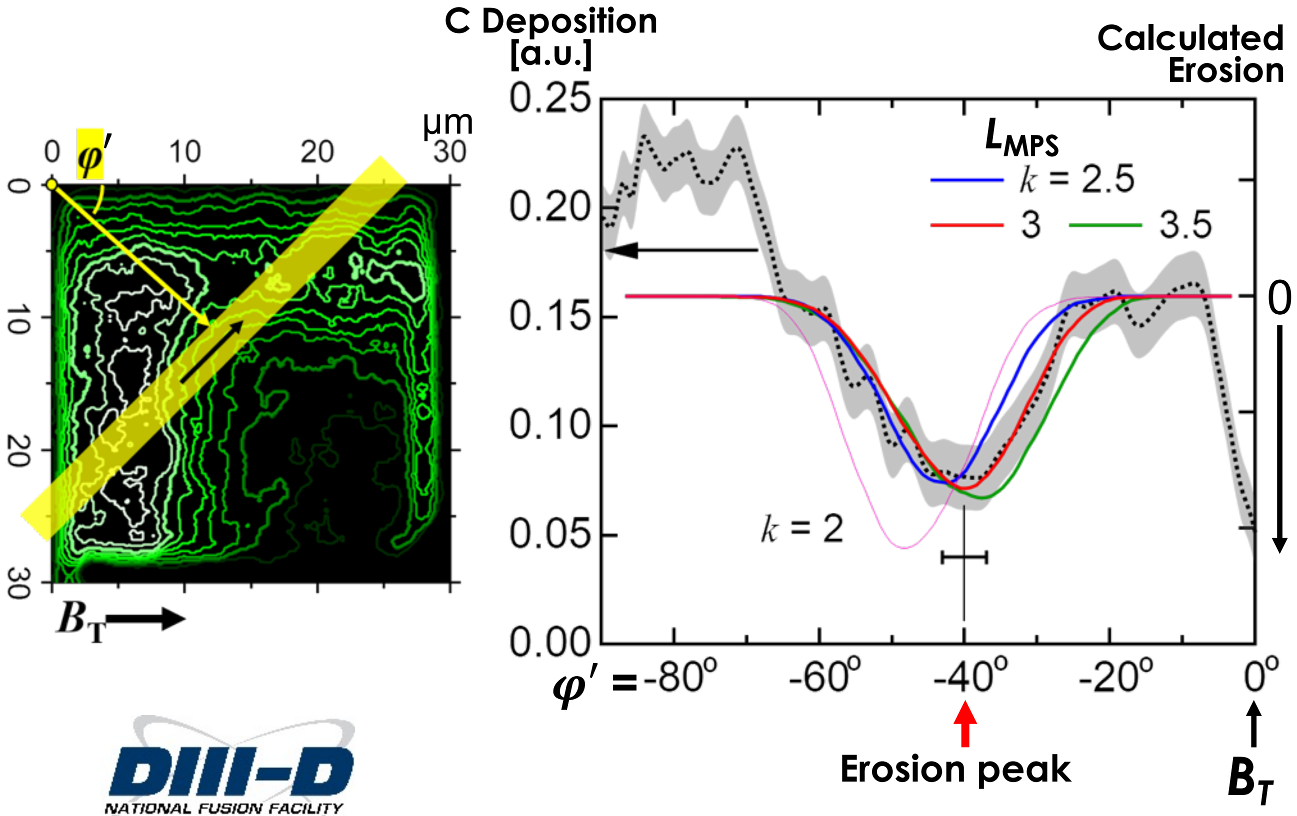

Good agreement is obtained for **k = 2.5-3.5**

$L_{MPS} = k \times \rho_i$ (ρ_i: Ion gyro radius)

giving azimuthal D ion direction

***φ* = -40°**

Abe, NF 2021 accepted

L_{MPS} (*k*) was determined by comparing with calculated erosion

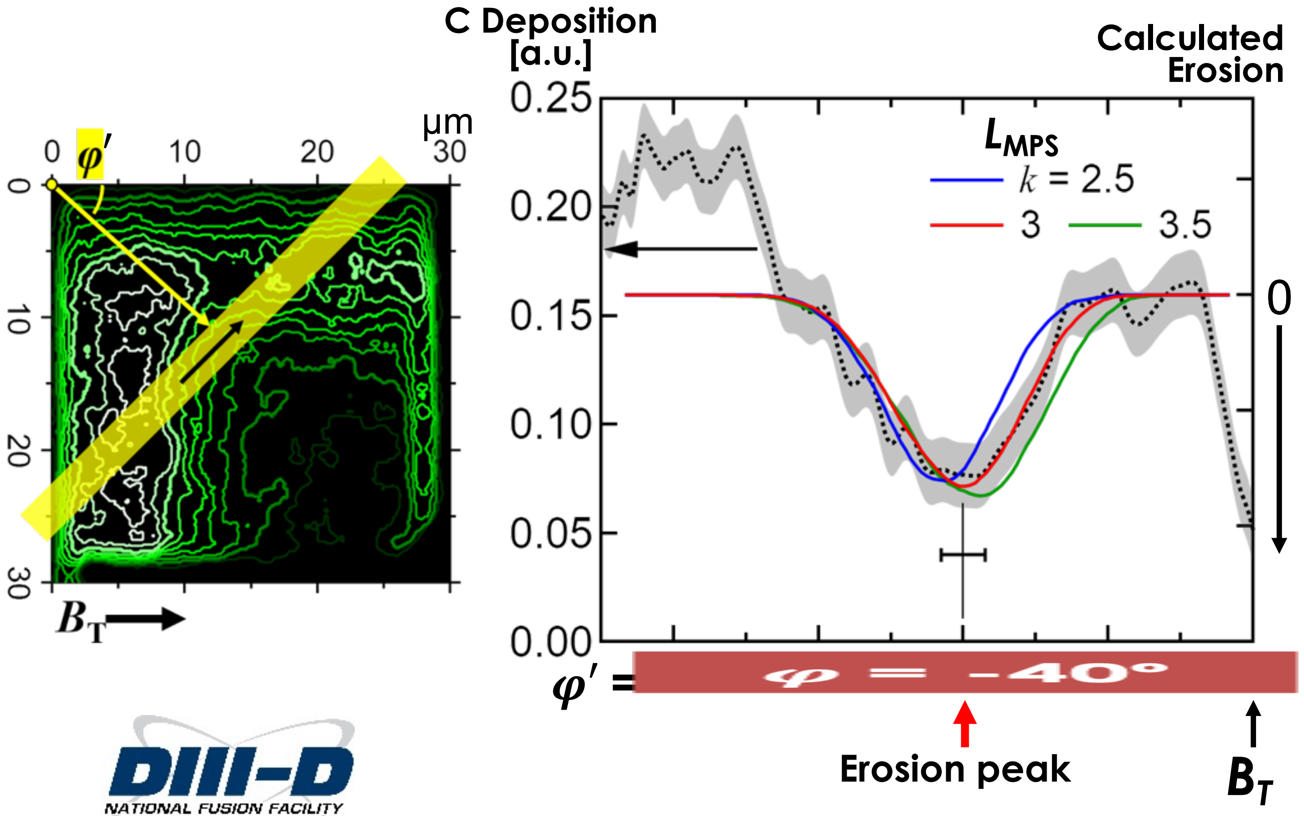

Good agreement is obtained for **k = 2.5-3.5**

$L_{MPS} = k \times \rho_i$ (ρ_i: Ion gyro radius)

giving azimuthal D ion direction

φ = -40°

Abe, NF 2021 accepted

... consistent with

***k* = 3** predicted by kinetic-model

DIII-D **ITER** **Coulette PPCF 2016**

DIII-D NATIONAL FUSION FACILITY SAN DIEGO

Polar IAD gives L_{MPS} consistent with measurement

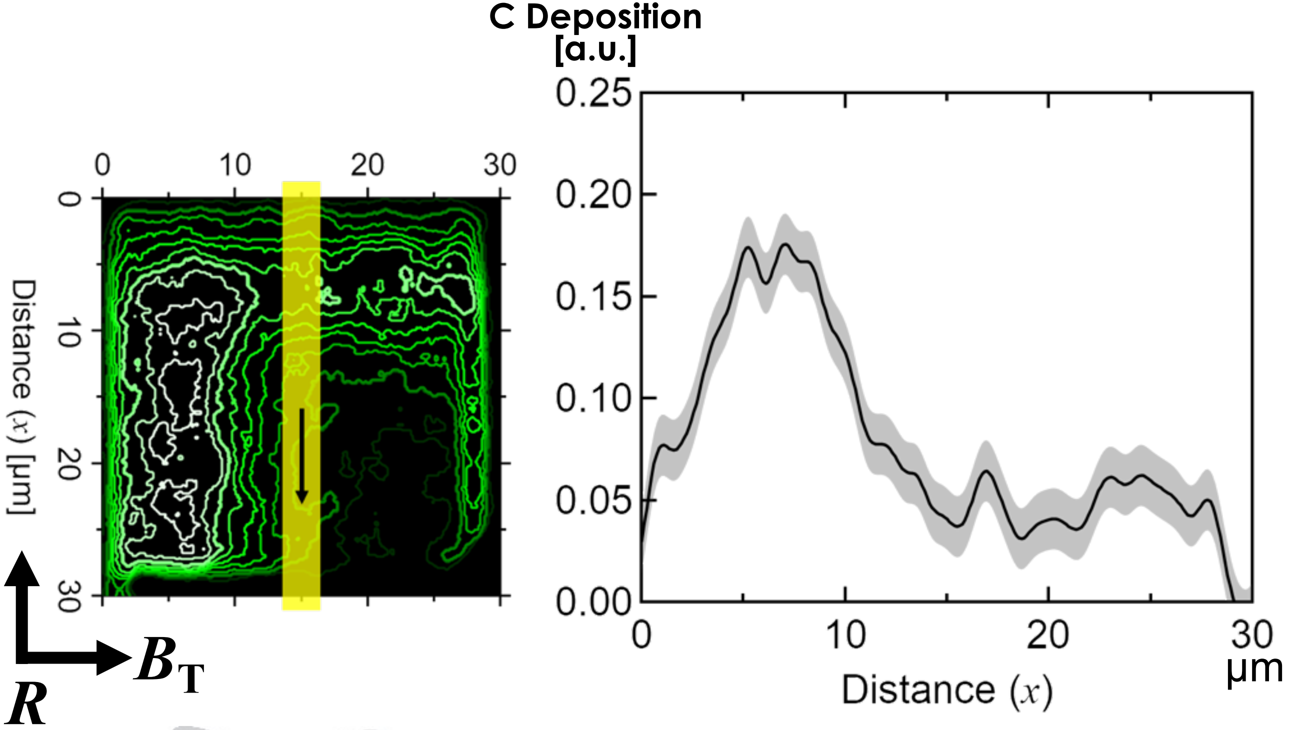

Polar IAD gives L_{MPS} consistent with azimuthal measurement

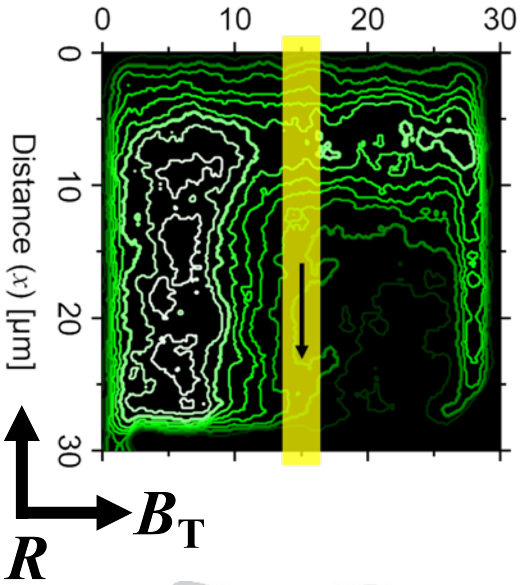

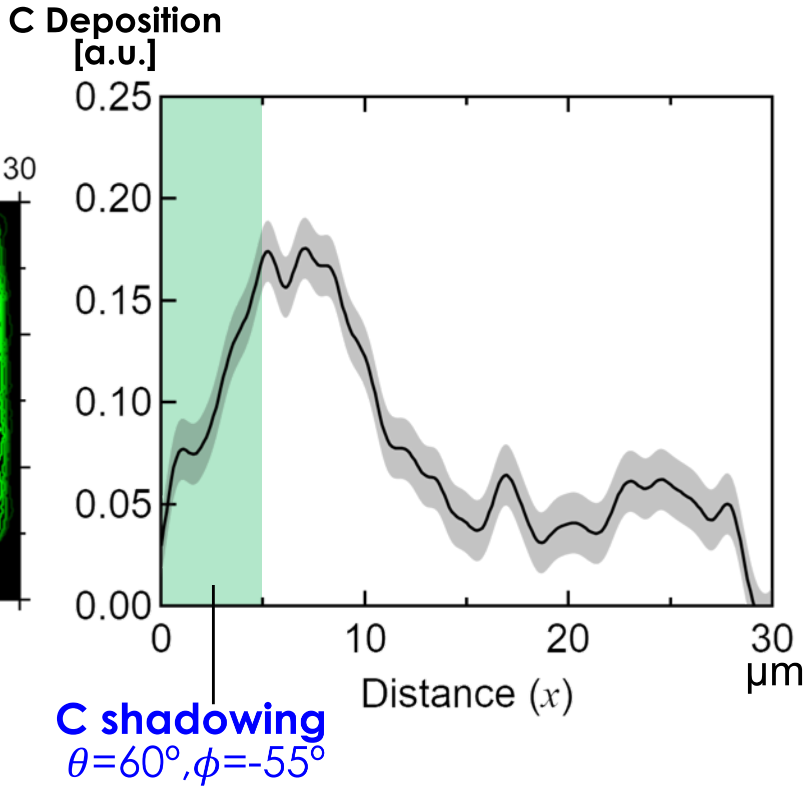

C ion shadowing 0-5 μm

- Consistent with C ion direction measured by micro-spheres
Bykov, unpublished

Polar IAD gives L_{MPS} consistent with azimuthal measurement

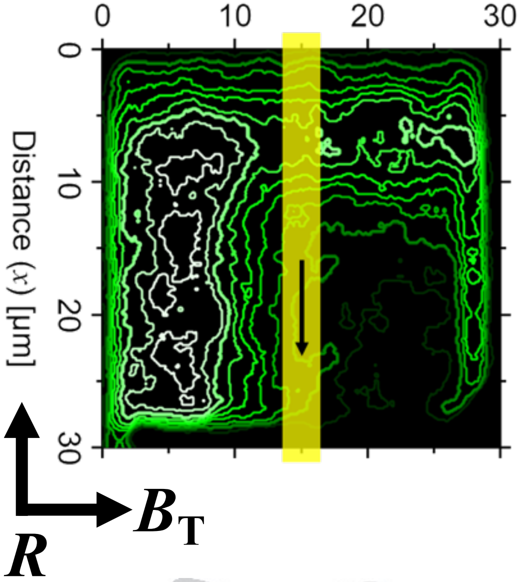

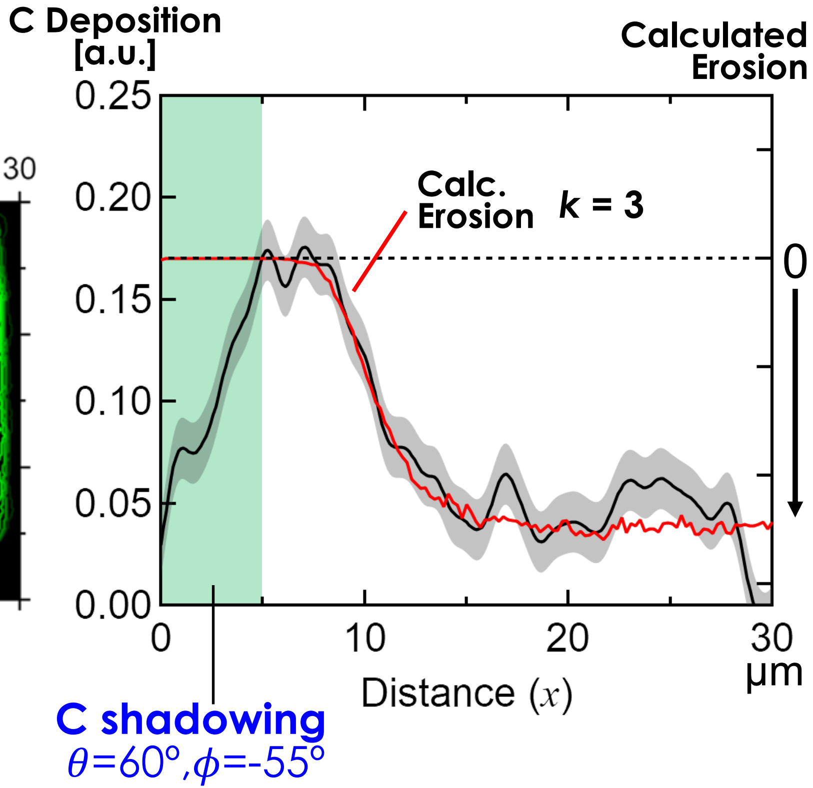

C ion shadowing 0-5 μm

- Consistent with C ion direction measured by micro-spheres
Bykov, unpublished

Polar IAD gives L_{MPS} consistent with azimuthal measurement

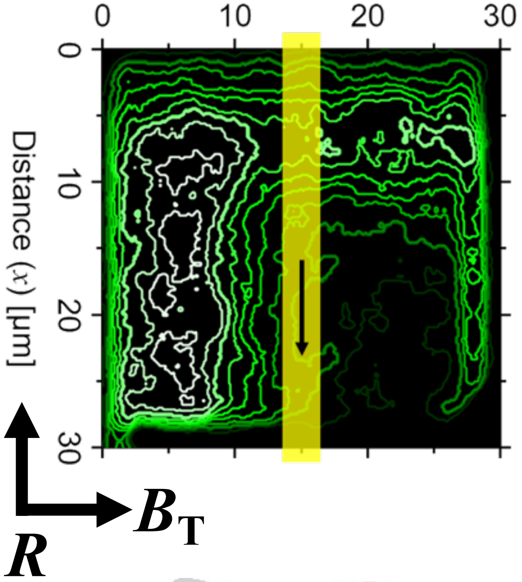

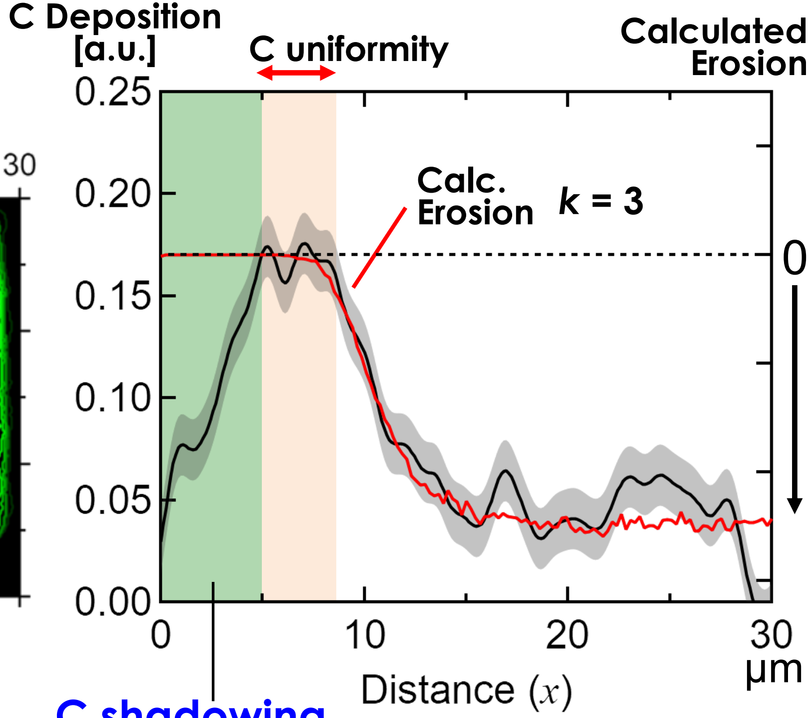

C shadowing
θ=60°,ϕ=-55°

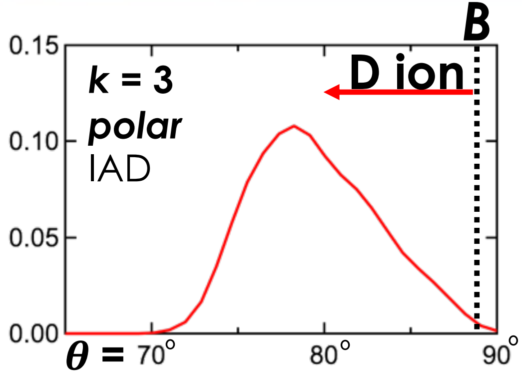

C ion shadowing 0-5 μm

- Consistent with C ion direction measured by micro-spheres
Bykov, unpublished

Uniformity is seen in D ion shadowed area 0-9 μm
(defined by θ ~ 70°)

DIII-D NATIONAL FUSION FACILITY SAN DIEGO

Polar IAD gives L_{MPS} consistent with azimuthal measurement

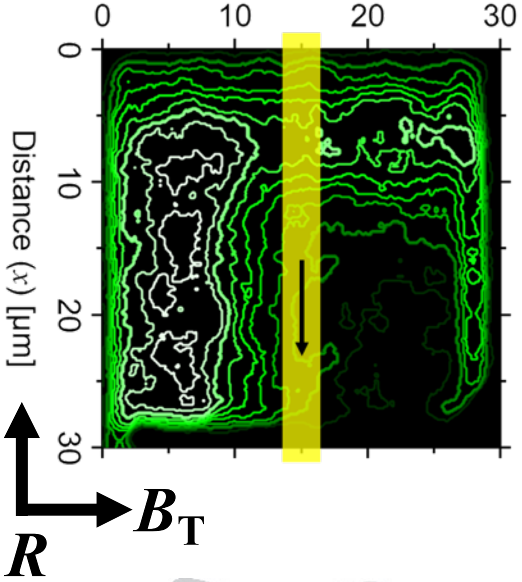

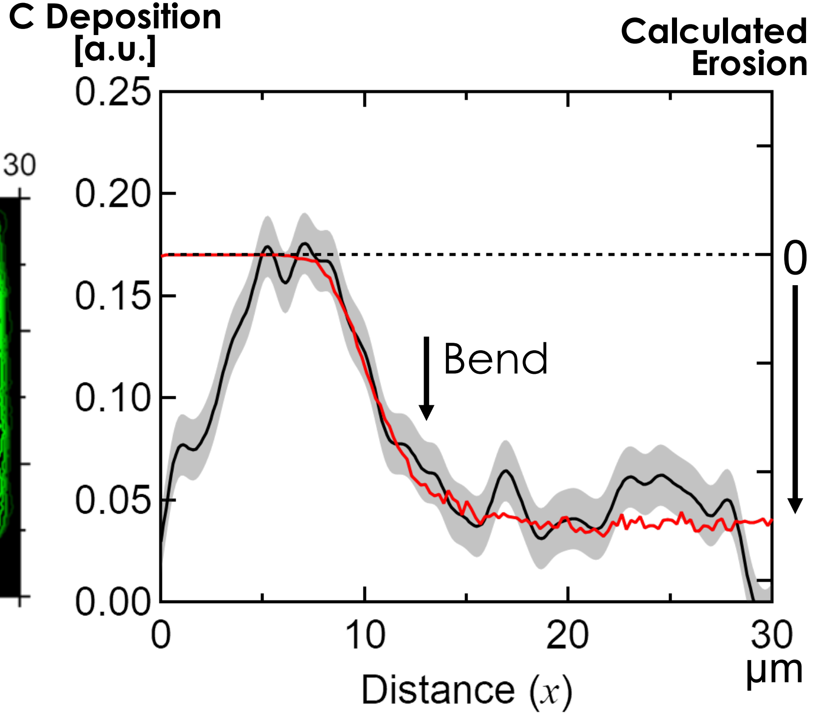

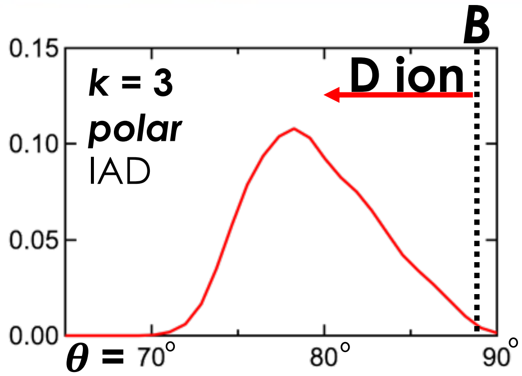

***k* = 3** IADs give a bend in erosion profile at 13 μm

- consistent with deposition profile

DIII-D NATIONAL FUSION FACILITY SAN DIEGO

Polar IAD gives L_{MPS} consistent with azimuthal measurement

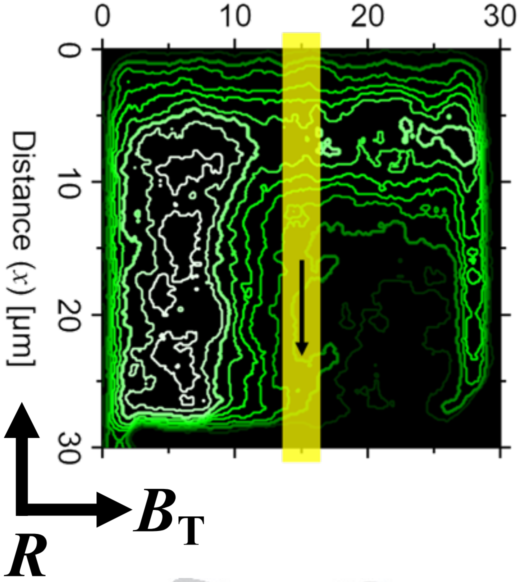

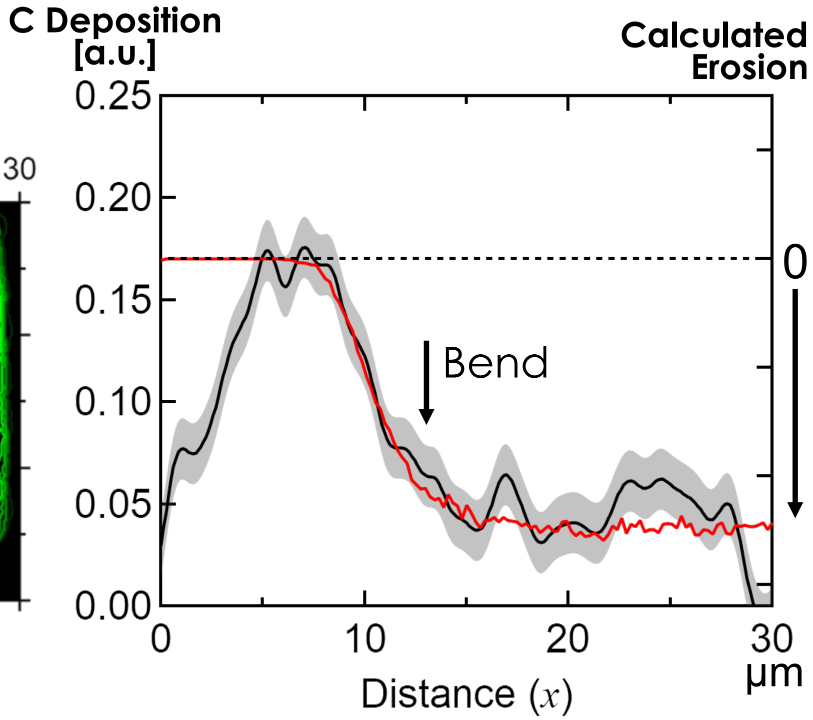

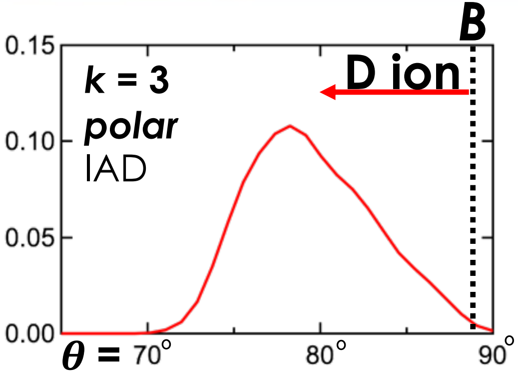

***k* = 3** IADs give a bend in erosion profile at 13 μm
- consistent with deposition profile

This agreement verifies

$\theta \sim 80°$

Polar IAD determination from **Abe NME 2021**

DIII-D NATIONAL FUSION FACILITY SAN DIEGO

Ga erosion can be a clue of the original trench surface erosion

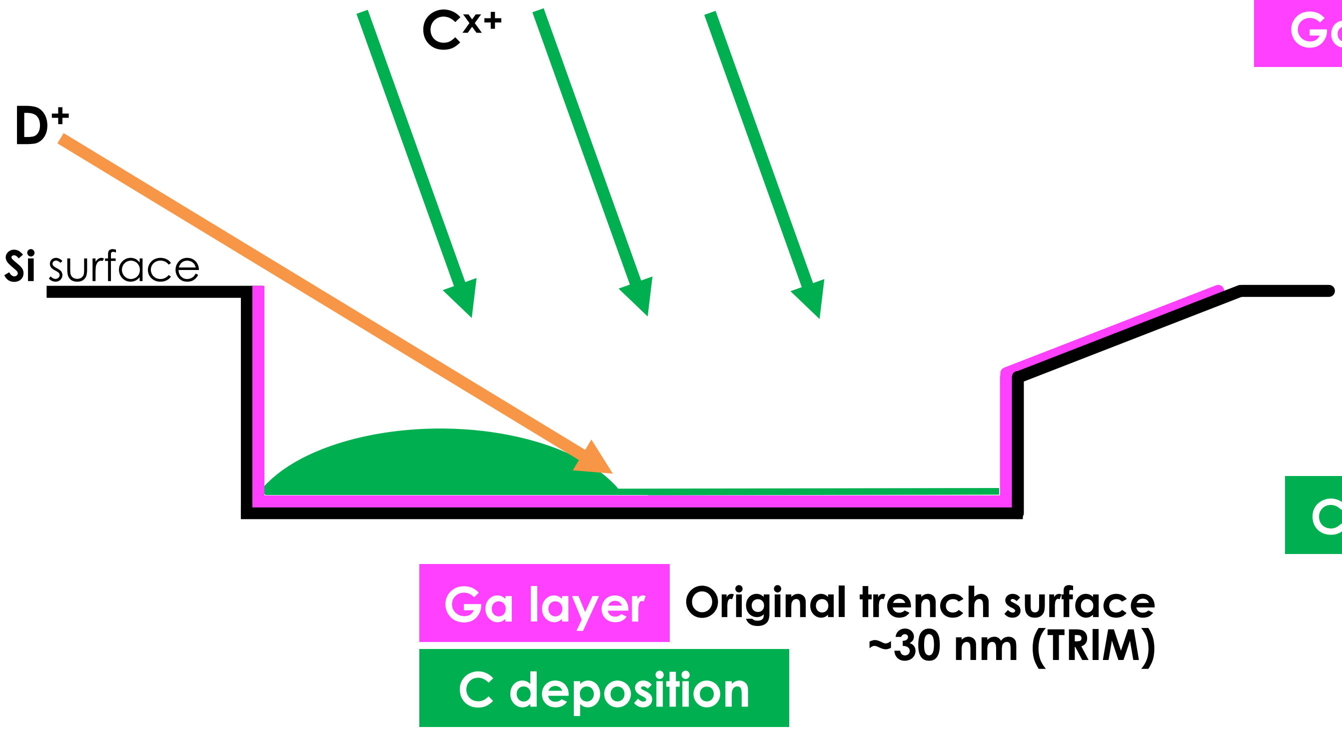

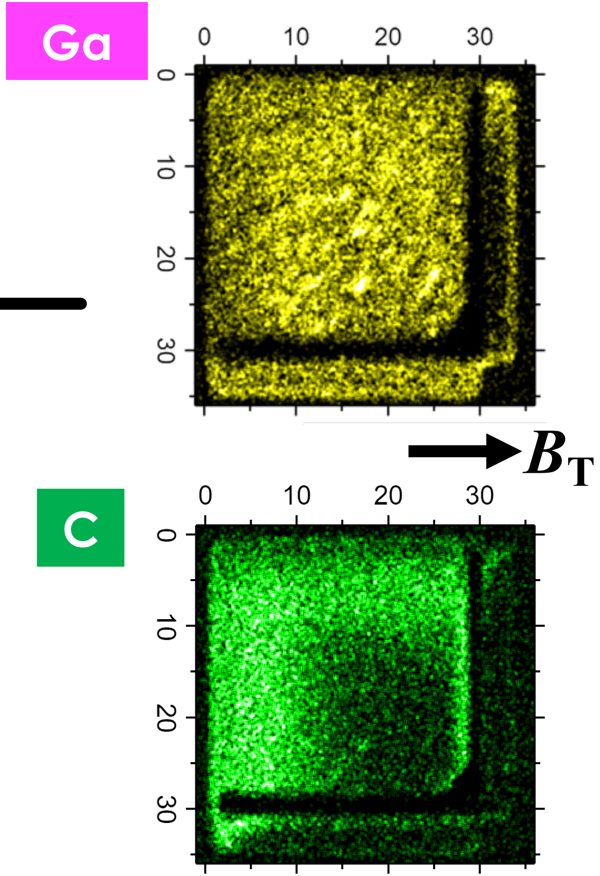

Ga erosion can be a clue of the original trench surface erosion

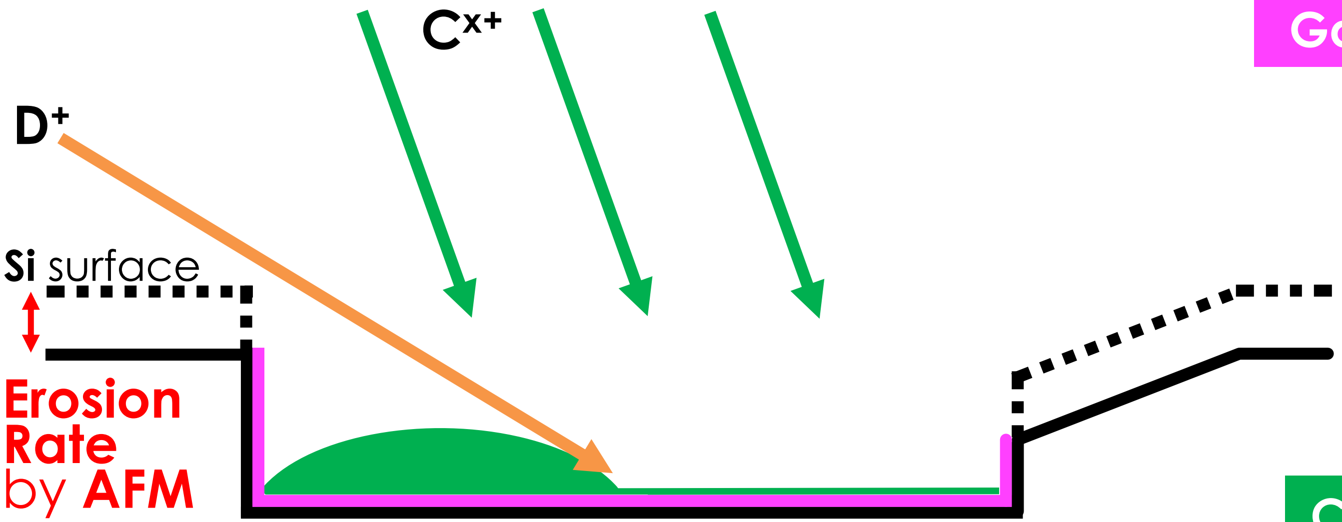

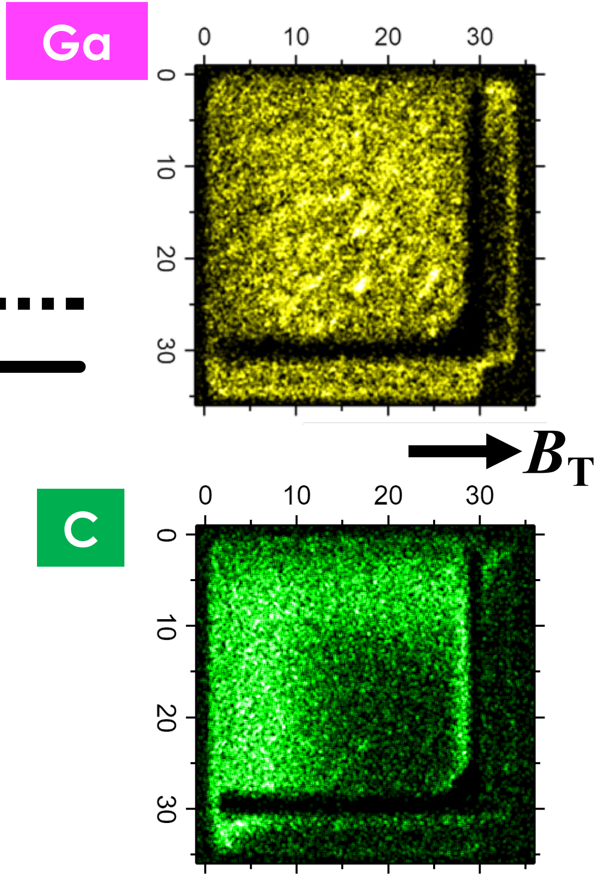

Reference → Ga layer Original trench surface ~30 nm (TRIM)

C deposition

Si erosion rate negatively correlates with C concentration

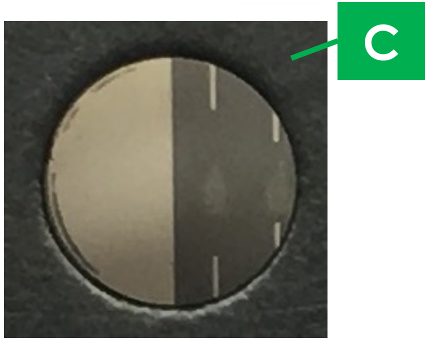

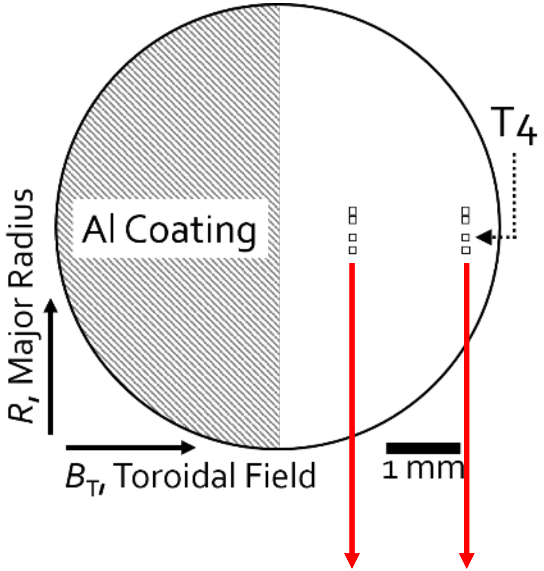

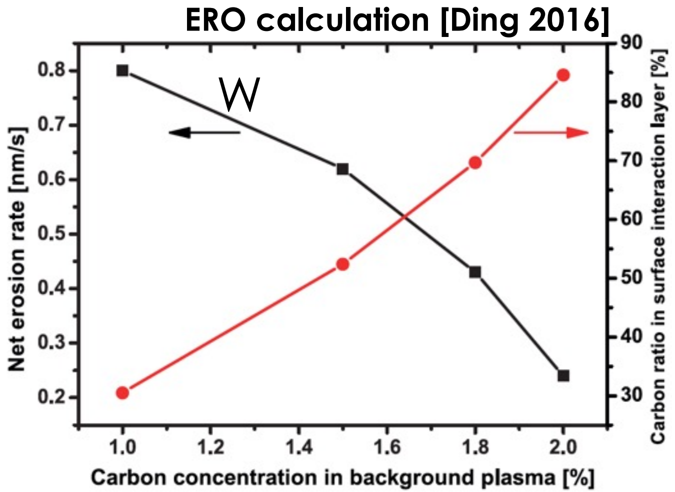

Si erosion rate	**5.5**	3.5 **nm/s**
C concentration	4.5	**5.4%**

C concentration reduces Si surface erosion

- **Surface dilution?**
- **SiC formation?**

DIII-D NATIONAL FUSION FACILITY SAN DIEGO

Si erosion rate negatively correlates with C concentration

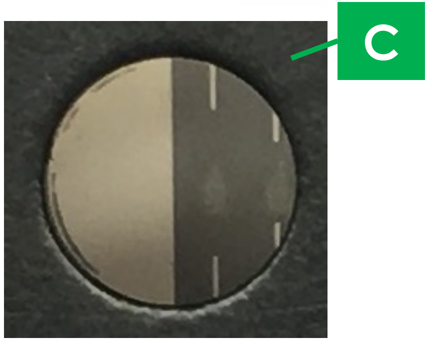

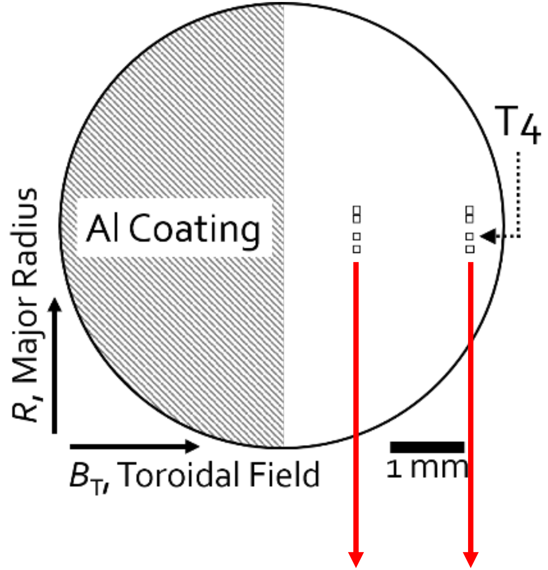

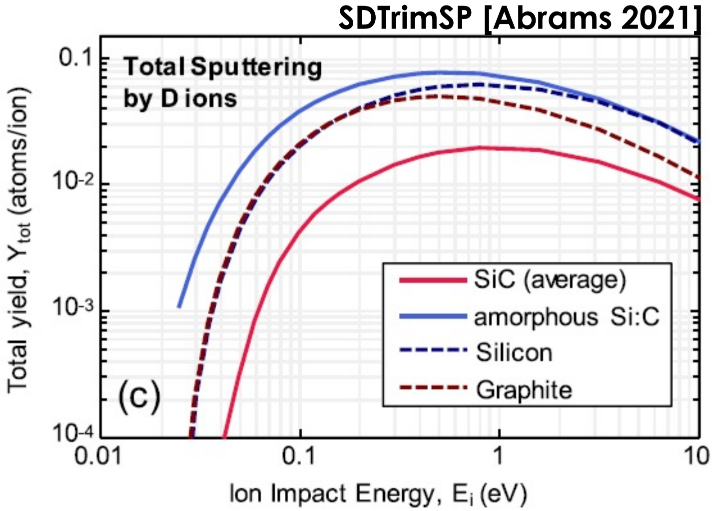

Si erosion rate	**5.5**	3.5 **nm/s**
C concentration	4.5	**5.4%**

C concentration reduces Si surface erosion

- **Surface dilution?**
- **SiC formation?**

What is the origin of the differential slope erosion?

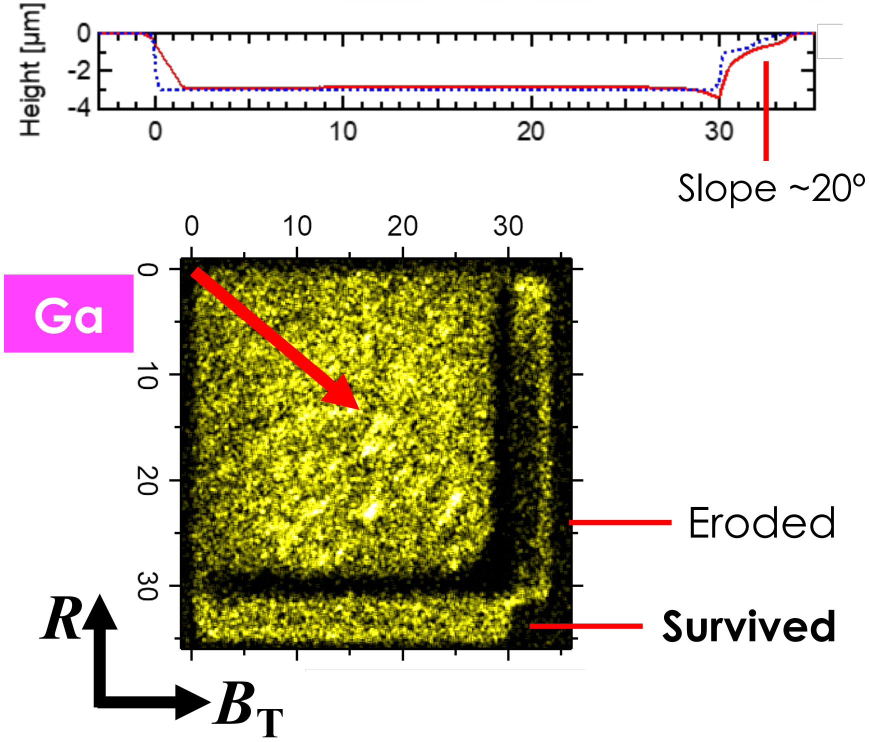

D ion direction

φ = -40° **(θ = 80°)**

D ion flux and incident angle (~65°) is almost same between both slopes

What is the origin of the differential slope erosion?

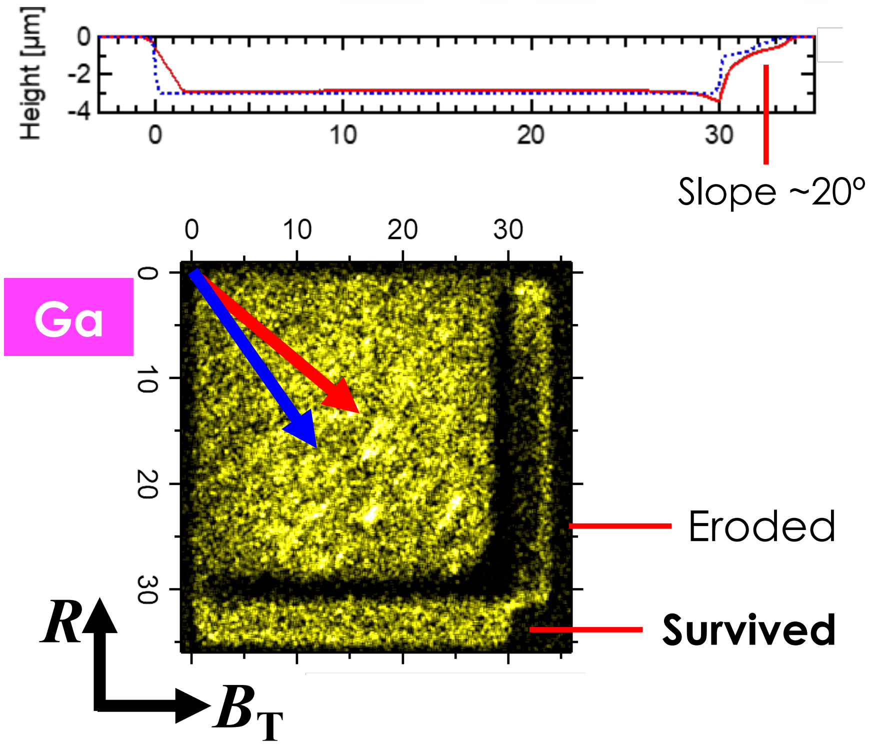

D ion direction

φ = -40° **(θ = 80°)**

D ion flux and incident angle (~65°) is almost same between both slopes

Impurity C ion direction

φ = -55° **(θ = 60°)**

measured by Bykov and calculated (ERO) by Guterl

→ can make the differential erosion by differential deposition

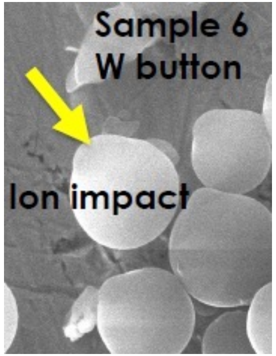

Bykov, unpublished

What is the origin of the differential slope erosion?

Impurity C ion direction

φ = -55°

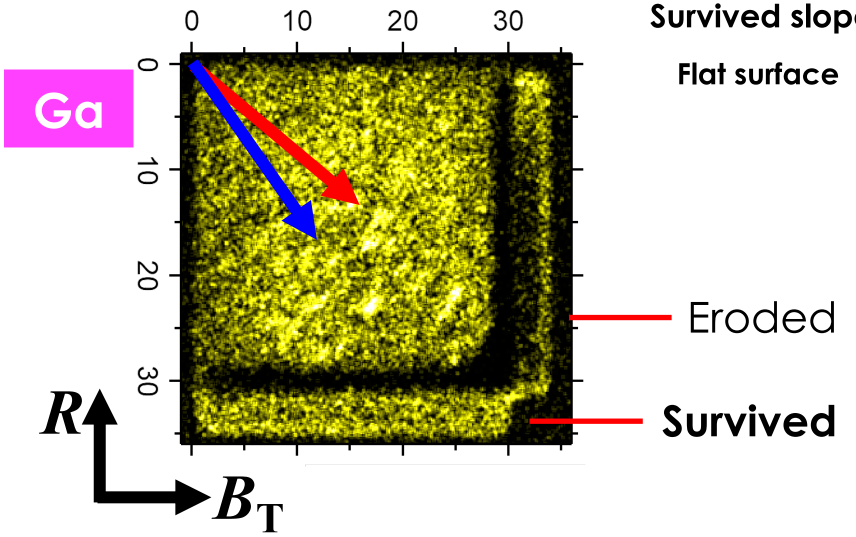

MPR calculation

	Impact Angle	Norm. Flux	C^+(140eV)→C Retention Yield [/ion]	C^+(140eV)→C Sputtering Yield [/ion]	C^+(140eV)→C Deposition Rate [a.u.]	C^{3+}(300eV)→C Retention Yield [/ion]	C^{3+}(300eV)→C Sputtering Yield [/ion]	C^{3+}(300eV)→C Deposition Rate [a.u.]
Eroded slope	48°	1.5	0.90	0.28	**0.93**	0.76	0.53	**0.35**
Survived slope	40°	1.7	0.95	0.19	**1.29**	0.81	0.37	**0.75**
Flat surface	60°	1	0.76	0.41	**0.35**	0.61	0.8	**-0.19**
			$1\text{-}R_N$	Y_{phys}		$1\text{-}R_N$	Y_{phys}	

Reflection yield

DIII-D NATIONAL FUSION FACILITY SAN DIEGO

What is the origin of the differential slope erosion?

Impurity C ion direction

$\varphi = -55°$

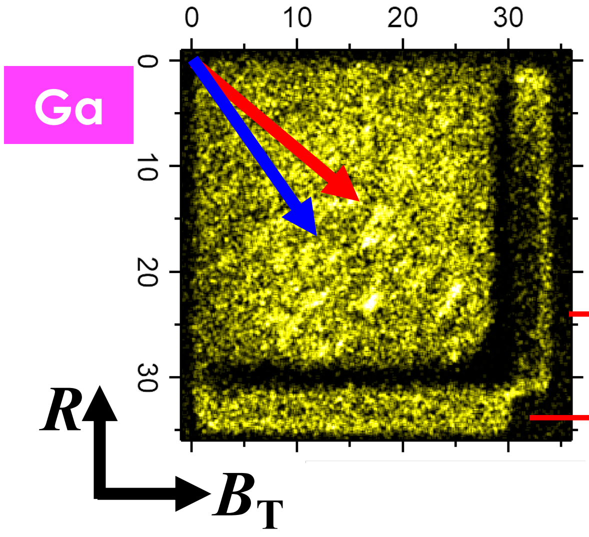

MPR calculation

	Impact Angle	Norm. Flux	C^{+}(140eV)→C Retention Yield [/ion]	C^{+}(140eV)→C Sputtering Yield [/ion]	C^{+}(140eV)→C Deposition Rate [a.u.]	C^{3+}(300eV)→C Retention Yield [/ion]	C^{3+}(300eV)→C Sputtering Yield [/ion]	C^{3+}(300eV)→C Deposition Rate [a.u.]
Eroded slope	48°	1.5	0.90	0.28	**0.93**	0.76	0.53	**0.35**
Survived slope	40°	1.7	0.95	0.19	**1.29** ←	0.81	0.37	**0.75** ←
Flat surface	60°	1	0.76	0.41	**0.35**	0.61	0.8	**-0.19**
			$1\text{-}R_N$	Y_{phys}		$1\text{-}R_N$	Y_{phys}	

C Effective Deposition Rate

$$= ((1 - R_N) - Y_{phys})*I_{ion}$$

Higher C deposition rate on the survived slope than eroded slope

140-210%

DIII-D NATIONAL FUSION FACILITY SAN DIEGO

What is the origin of the differential slope erosion?

Impurity C ion direction

φ = -55°

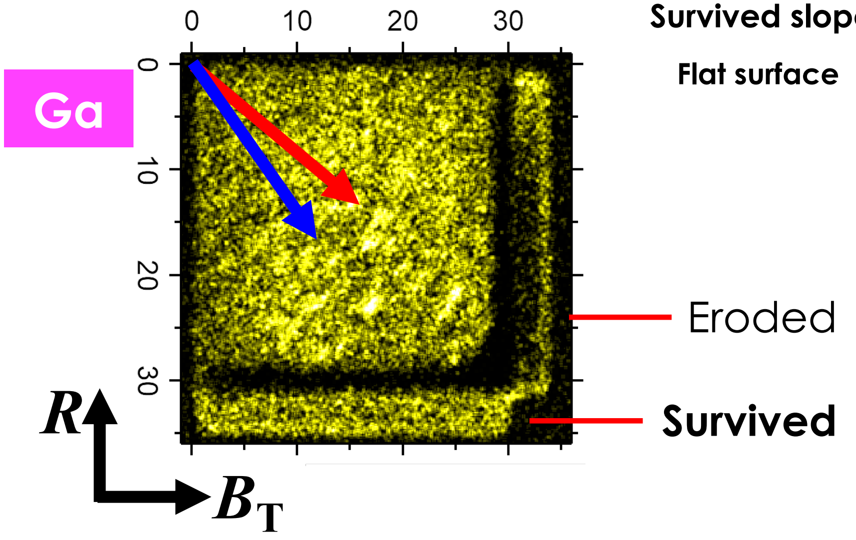

MPR calculation

	Impact Angle	Norm. Flux	C^+(140eV)→C Retention Yield [/ion]	C^+(140eV)→C Sputtering Yield [/ion]	C^+(140eV)→C Deposition Rate [a.u.]	C^{3+}(300eV)→C Retention Yield [/ion]	C^{3+}(300eV)→C Sputtering Yield [/ion]	C^{3+}(300eV)→C Deposition Rate [a.u.]
Eroded slope	48°	1.5	0.90	0.28	**0.93**	0.76	0.53	**0.35**
Survived slope	40°	1.7	0.95	0.19	**1.29** ←	0.81	0.37	**0.75** ←
Flat surface	60°	1	0.76	0.41	**0.35**	0.61	0.8	**-0.19**
			$1-R_N$	Y_{phys}		$1-R_N$	Y_{phys}	

C Effective Deposition Rate

$$= ((1 - R_N) - Y_{phys}) * I_{ion}$$

Higher C deposition rate on the survived slope than eroded slope

140-210%

Measured concentration [%]	C	Ga
Eroded slope	6.4 ±0.5	0.7 ±0.4
Survived slope	9 ±1	4.7 ±0.4

DIII-D NATIONAL FUSION FACILITY SAN DIEGO

What is the origin of the differential slope erosion?

Impurity C ion direction

φ = -55°

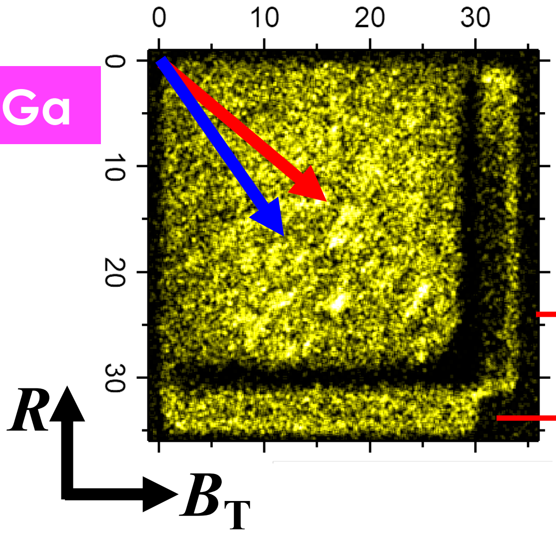

MPR calculation

	Impact Angle	Norm. Flux	C^+(140eV)→C Retention Yield [/ion]	C^+(140eV)→C Sputtering Yield [/ion]	C^+(140eV)→C Deposition Rate [a.u.]	C^{3+}(300eV)→C Retention Yield [/ion]	C^{3+}(300eV)→C Sputtering Yield [/ion]	C^{3+}(300eV)→C Deposition Rate [a.u.]
Eroded slope	48°	1.5	0.90	0.28	**0.93**	0.76	0.53	**0.35**
Survived slope	40°	1.7	0.95	0.19	**1.29** ←	0.81	0.37	**0.75** ←
Flat surface	60°	1	0.76	0.41	**0.35**	0.61	0.8	**-0.19**
			$1-R_N$	Y_{phys}		$1-R_N$	Y_{phys}	

C Effective Deposition Rate
$$= ((1 - R_N) - Y_{phys}) * I_{ion}$$

Higher C deposition rate on the survived slope than eroded slope

140-210%

Impurity C (even for few %) incident angle is also important for erosion

Abe, Phys. Scr. 96 2021

DIII-D NATIONAL FUSION FACILITY SAN DIEGO

Summary

- D ion azimuthal direction is $\boldsymbol{\varphi}$ **= -40°** where B field was referenced to $\boldsymbol{\varphi}$ = 0°, and polar peak angle is $\boldsymbol{\theta}$ ~ **80°** (B field: $\boldsymbol{\alpha}$ = 88.5°)
- Comparison with MPR gross erosion calculation verified the sheath scale width factor ***k*** **= 2.5-3.5** ($L_{MPS} = k \times \rho_i$, ρ_i: Ion gyro radius)
- Good agreement with kinetic-model prediction ***k*** **~ 3 for DIII-D and ITER parameters**
- C impurity concentration and incident angle are important parameters for erosion

Acknowledgements

Acknowledgement: BEK (PU) group, C. Chrobak, R. Akhmechet, Z. Lewicka, D. Barth, J. Schreiber, G. Cheng, D. Buchenauer, J. Whaley, R. Kolasinski, F. Zhao, B. Harrop, D. Coulette, G. Manfredi

This work from **S. Abe et al.** **2021 Nucl. Fusion, accepted**
2021 Phys. Scr. 96 124039
2021 Nucl. Mater. Energy 27 100965

PPPL: DE-AC02-09CH11466
DIII-D: DE-FC02-04ER54698
LLNL: DE-AC52-07NA27344
UCSD: DE-FG02-07ER54917

DIII-D NATIONAL FUSION FACILITY SAN DIEGO
PRINCETON UNIVERSITY
PPPL